

Interactive comment on “Reduction in Earth Reflected Radiance during the Eclipse of 21 August 2017” by Jay Herman et al.

Anonymous Referee #2

*Based on your comments, I have made a lot of changes to the text and calculations in the paper. All changes are indicated in **GREEN**. The altered version is attached at the end.*

Received and published: 27 March 2018

The authors use DISCOVER/EPIC observations from 21st August 2017, which were taken in the Lagrange-1 point, to estimate the reduction of Earth reflected solar radiance during the solar eclipse. They compare images from the day before and the day after the eclipse and find a reduction of about 9.7% for a particular location (Casper, Wyoming). They find similar results for absorbing and non-absorbing channels, thus they conclude that the reflected energy is dominated by radiation reflected by clouds with a significant contribution of Rayleigh scattering at the shorter wavelengths. Further, for two locations, they have calculated the reduction of reflected radiance in the totality region and they found, that it highly depends on the cloud cover. When clouds are present, the reduction is much less than without clouds.

Since this is to my knowledge the first estimate of the reduction of the reflected radiance from space, the result is interesting and it should be published.

However, before publication in AMT, the paper needs to be revised and some figures could be improved (see below).

General comments:

1. In the abstract and also later in the text (l. 237 ff, l. 366 ff), the observations are compared to modelling results by Emde and Mayer, 2007: "A previously published clear-sky model (Emde and Mayer, 2007) shows results for a nearly overhead eclipse had $R_{EN}(340nm)=1.7 \times 10^{-4}$ compared to the maximum measured non-averaged $R_{EN}(340)$ at Casper of 515 ± 27 with optically thin clouds under similar geometrical conditions." Such a quantitative comparison is not possible, because the modelling result refers to the reduction of global irradiance (measured from the surface) in the center of the umbral shadow. This is a different quantity and the observation geometry is completely different, thus it is not surprising that the results do not agree to the DISCOVER observations. For a quantitative comparison, the 3D radiative transfer model needs a completely different setup, one has to model the reflected radiance for the specific observation geometry of DISCOVER (with a phase angle of about 172°). This should be possible using a Monte Carlo code like MYSTIC used by Emde and Mayer, 2007, but as said before, it requires a completely different setup. It can be mentioned in the text, that it would be interesting to model the observations with 3D RT models, but quantitative comparisons should be removed from abstract, text and summary.

2. Why is the global reduction of the reflectance (Section 3.2) only calculated for Casper and not

for Columbia. It would be interesting to see, how much the reduction of global reflectance depends on the location of the clouds. Please include results for Columbia in Section 3.2.

I have added the Columbia calculation. It is almost the same as the Casper calculation, since the earth's cloud cover did not change much in the short time interval between the eclipse at Casper and Columbia.

3. Could the DISCOVER data, which is used for the study, added as supplementary data to the paper in addition to the provided links?

The data are available freely from https://eosweb.larc.nasa.gov/project/dscovr/dscovr_epic_l1b, but I will try to upload the data files with some extra documentation.

Specific comments:

I.1 "Sunlit" -> "sunlit" **OK**

I. 16: "A reduction of $9.7 \pm 1.7\%$ in the radiance (387 to 781 nm) reflected from the Earth towards L1 was obtained..." -> Please clarify that this is the spectrally integrated global reflectance.

OK

I. 25ff: "A previously published ..." -> remove this sentence from abstract (see above). I.45

"earth" -> "Earth" **OK**

I. 55: "The totality region (umbra) is about 250 to 267 km in diameter, ..." -> in line 151 it is said that the totality shadow is 116 km wide over Caspar. How do these numbers match?

Fixed. My mistake

In I. 151ff both axes of the umbral shadow should be provided for both locations (Casper and Columbia). On which parameters does the size of the shadow depend apart from solar zenith angle? The distances Sun-Earth, Moon-Earth also determine the extent of the shadow.

I changed the sentence to read: "The totality region (umbra) is an oval of about 110 -120 km in size near local noon at Casper, Wyoming and Columbia, Missouri, but will change size and shape as a function of local solar zenith angle (<https://eclipse2017.nasa.gov/eclipse-maps>)."

The umbral size does depend a little on the Sun-Earth distance, but for this particular eclipse, the size just depends on the local solar zenith angle.

I. 60ff: The overview paper of Gerasopoulos et al., 2008 is cited and it is said that it would include MODIS observations of the eclipse from 2006 over Europe. This is not correct, the paper includes a MODIS image from the same day (taken before eclipse) to show the cloud formation over Greece.

That is correct. I changed the sentence to read: ".....observations of cloud cover before totality (Gerasopoulos et al., 2008)...."

I.66ff: "A 3D Monte Carlo radiative transfer study (Emde and Mayer, 2007) was applied to the geometry for the nearly overhead total eclipse of 29 March 2006 (13:20 local time in Turkey), but without the effect of clouds included in the calculation. Successful modelling of an eclipse

under realistic conditions is the first step to improved modelling ..." -> The modelling was realistic for the given observation over Greece, because the region was cloud-free. A comparison to observations showed an excellent agreement (see Kazantzidis et al. 2007, <https://www.atmos-chem-phys.net/7/5959/2007/>). Of course, clouds need to be included when present. Please clarify this sentence.

Thank you. I missed that reference. I added the sentence: "The 3D model showed good agreement with fairly cloud-free (few cumulus, 1-2 octas, and scattered cirrus, 3-4 octas) measurements at 380 nm of the ratio of global irradiance starting 5 minutes before totality to that during totality (Kazantzidis et al., 2007)."

I. 71ff: "The observations from the DSCOVR satellite are part of a larger project that combines simultaneously obtained satellite and ground-based measurements using a pyranometer (Ji and Tsay, 2000) and the Pandora Spectrometer Instrument (Herman et al., 2009) at both sites." -> Is this data available?

The data are available, but is the subject of another paper by Guoyong Wen, the main investigator for the project.

I. 75: "This study presents the only synoptic satellite data of the sunlit Earth ever obtained during an eclipse ..." -> What about images from geostationary satellites? I remember movies of MSG images of the eclipse from March 2006.

You are correct about images, but not spectral calibrated data. I added the word spectral.

"This study presents the only calibrated spectral synoptic satellite data of the sunlit Earth ever obtained during an eclipse".

I.119: "To reduce the volume of data, all measurements, except those from the 443 nm channel, were averaged onboard DSCOVR to 1024 x 1024 pixels." -> Why is the 443nm channel treated differently?

The EPIC project wanted at least one high resolution channel to help with geolocation of the images and to enhance the resolution of the RGB color pictures.

I. 167: "340 nm, with strong Rayleigh scattering effects (haze)" -> haze (aerosol) scattering is not the same as Rayleigh (molecular) scattering.

I should not have used the word haze – I was using it subjectively. It has been removed

Fig.3: These images are very nice. I would prefer north up as usual, even if inconsistent with Fig. 7. **I usually prefer north up, but went for consistency instead. If it is really important, I can rotate the figures with north up.**

I. 173 "3.1 Comparison of Eclipse and Non-Eclipse Days for Caspar, WY and Columbia, MO "-> Use a more specific title, what is compared?

It's a bit long, but: "Comparison of EPIC Observations of Eclipse Totality (21 Aug) with Non-Eclipse

Days (20 and 23 Aug) for Casper, WY and Columbia, MO.

Fig. 5: "Middle"-> "Bottom" **Fixed. The original figure had an addition row**

Fig. 6a,b: These figures all look quite similar. Why are all channels shown for Caspar, WY and only one for Columbia (as lower left plot in Fig 6a). This arrangement is confusing. Suggestion: Use 3 representative channels and show the results for Caspar, WY on the left and the corresponding results for Columbia on the right. Maximum values for all channels and for both locations should be included in Table 2.

I calculated the results for all 10 channels for both Casper and Columbia, but did it differently than in the original document. In the original document I used a Lowess running average of 12 data points to produce a smooth curve. I forgot to add that to the figure caption, but it was in the text. In the present version, I am showing the original data points with no spatial averaging. The maximum values are shown in the figures and Table 2.

Table 2: Please include also the <R_EN> values for Columbia in the table. **OK**

I. 234ff: "A detailed radiative transfer study for realistic conditions is made feasible by using EPIC's simultaneous estimates of cloud reflectivity and transmission, cloud height, aerosol amounts, and ozone amounts." -> Is there a data product including these estimates. If yes, please provide reference.

Ozone, cloud reflectivity, and cloud transmission:

Herman, Jay, Liang Huang, Richard McPeters, Jerry Ziemke, Alexander Cede, and Karin Blank, Synoptic ozone, cloud reflectivity, and erythemal irradiance from sunrise to sunset for the whole earth as viewed by the DSCOVR spacecraft from the earth–sun Lagrange 1 orbit, 2017, Atmos. Meas. Tech., 10, 1–18, <https://doi.org/10.5194/amt-10-1-2017>.

OK I added an ozone figure in the appendix.

I am not sure if the aerosol paper has been published yet. The lead author will be Omar Torres.

I. 237ff: see "general comment 1"

Fig.8 a,b,c, A2: I think that not all of these figures are needed. Fig. 3 nicely shows, how the shadow and the Earth looks in various channels and Fig. 4 shows the synoptical conditions during the eclipse and the day before and after the eclipse. I suggest to put most of these

figures in the appendix.

The figures for 340 and 388 nm have been moved to the appendix. The main conclusion of this paper is based on a ratio of data from 20 Aug and 21 Aug. Most of the contribution to reflected radiances comes from the 443, 551, 680, and 780 nm channels.

I. 285: "While the figures are similar from wavelength to wavelength, there are differences in the depth of the eclipse totality and the reflectivities of the surrounding clouds." With the chosen grey-scale colormaps these difference are not visible. I suggest to use a colormap similar to the one in Fig.7 to visualize the differences in the depth of the eclipse totality.

I was asked by the editor after the original submission to show all of the wavelengths in a form where you could see the land areas. I was unable to do this in color contour plots, but could do it in greyscale.

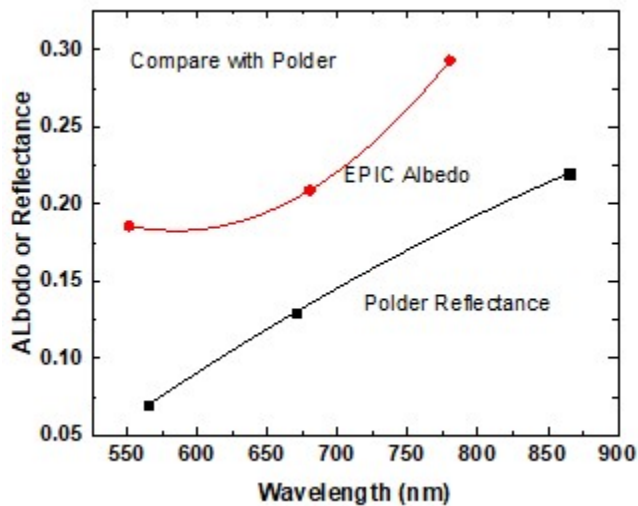
Table 3: Please include this table also for Columbia. **OK**

I. 325: "This means that EPiC is observing close to "hotspot" conditions where the backscatter amount increases with increasing wavelength (Maignan et al., 2004). At 551 and 680 nm the hotspot effect is smaller than at 780 nm." -> This is not obvious from Table 3, integrated counts are much larger for 551nm than for 780nm. Please explain.

The results appear to be in contrast to measurements from Polder (Maignan et al., 2004), which show increasing reflectivity with increasing wavelength over northern China. There are two main differences in the EPiC data (Table 3). First, the data are measured $C/s(\lambda)$ that are basically raw radiance measurements proportional to the solar irradiance wavelength dependence (decreases with increasing wavelength after about 550 nm). Second, the Polder measurements are surface reflectances over land, where reflectivity of the surface increases at longer wavelengths. EPiC is measuring top of the atmosphere radiances (in C/s) that can be converted to top of the atmosphere reflectances using the calibration coefficients. In addition, the numbers in Table 3 are for a mixture of land and oceans.

The TOA eclipse measurements made by EPiC are near the backscatter direction (172°) for the incident solar irradiance over nearly cloud-free scenes. For land surfaces, such as the observations made at Casper and Columbia, measurements from the POLDER satellite over China show that the backscatter amount from the land surface increases with increasing wavelength (Maignan et al., 2004). For EPiC data over land that are comparable to the POLDER measurements, the C/s data should be converted to reflectance. When this is done, the wavelength dependence of EPiC is similar to POLDER even though there is no atmospheric correction and there is some cloud cover.

To directly answer your question I plotted the POLDER reflectance and the EPiC albedo for 172° backscatter.



I. 330: "The solar spectrum used is a combination of data named atlas_plus_modtran (Mayer and Kylling, 2005)." -> Mayer and Kylling is the reference for the libRadtran software package, from which the solar irradiance data is taken. Please rewrite sentence more clearly.

I. 363: "A previously published clear-sky model result for a nearly overhead eclipse ratios and an ocean surface albedo of 0.06 (Emde and Mayer, 2007) had $R_{EN}(340nm)=1.7 \times 10^{-4}$ compared to the measured non-averaged $R_{EN}(340)$ at Casper of 515 ± 27 with optically thin clouds under similar geometrical conditions." -> these results can not be compared (see general comments). Not R_{EN} has been modelled by Emde and Mayer, the value refers to global irradiance at the surface!

The sentence has been modified to: "A previously published **downward global surface radiation** clear-sky model result for a nearly overhead eclipse ratios..."

1 Reduction in sunlit Earth reflected radiance 317 to 780 nm during the eclipse of 21 August 2017

2 Jay Herman¹, Guoyong Wen², Alexander Marshak³, Karin Blank³, Liang Huang⁴, Alexander Cede⁵, Nader
3 Abuhassan¹, Matthew Kowalewski⁶

4 Abstract

5 Ten wavelength channels of calibrated radiance image data from the sunlit Earth are obtained
6 every 65 minutes during Northern Hemisphere summer from the DSCOVR/EPIC instrument located near
7 the Earth-Sun Lagrange-1 point (L_1), 1.5 million km from the Earth. The L_1 location permitted seven
8 observations of the Moon's shadow on the Earth for about 3 hours during the 21 August 2017 eclipse.
9 Two of the observations were timed to coincide with totality over Casper, Wyoming and Columbia,
10 Missouri. Since, the solar irradiances within 5 channels ($\lambda_i = 388, 443, 551, 680, \text{ and } 780 \text{ nm}$) are not
11 strongly absorbed in the atmosphere, they can be used for characterizing eclipse reduction in reflected
12 radiances for the sunlit face of the Earth containing the eclipse shadow. Five channels ($\lambda_i = 317.5, 325,$
13 $340, 688, \text{ and } 764 \text{ nm}$) that are partially absorbed in the atmosphere give consistent reductions
14 compared to the non-absorbed channels. This indicates that cloud reflectivities dominate the 317.5 to
15 780 nm radiances reflected back to space from the sunlit Earth's disk with a strong contribution from
16 Rayleigh scattering for the shorter wavelengths. A reduction of 10 % in the spectrally integrated
17 radiance (387 to 781 nm) reflected from the sunlit Earth towards L_1 was obtained for two sets of
18 observations on 21 August 2017, while the shadow was in the vicinity of Casper, Wyoming ($42.8666^\circ \text{ N},$
19 106.3131° W , centered on 17:44:50 UTC) and Columbia, Missouri ($38.9517^\circ \text{ N}, 92.3341^\circ \text{ W}$, centered on
20 18:14:50 UTC). In contrast, when non-eclipse days (20 Aug. and 23 Aug.) are compared for each
21 wavelength channel, the change in reflected light is much smaller (less than 1 % for 443 nm compared to
22 9 % (Casper) and 8 % (Columbia) during the eclipse). Also measured was the ratio $R_{EN}(\lambda_i)$ of reflected
23 radiance on adjacent non-eclipse days divided by radiances centered in the eclipse totality region with
24 the same geometry for all 10 wavelength channels. The measured $R_{EN}(443 \text{ nm})$ was smaller for Columbia
25 (169) than for Casper (935), because Columbia had more cloud cover than Casper. $R_{EN}(\lambda_i)$ forms a useful
26 test of 3-D radiative transfer models for an eclipse in the presence of optically thin clouds. Specific
27 values measured at Casper with thin clouds are $R_{EN}(340 \text{ nm}) = 475, R_{EN}(388 \text{ nm}) = 3500, R_{EN}(443 \text{ nm}) =$
28 $935, R_{EN}(551 \text{ nm}) = 5455, R_{EN}(680 \text{ nm}) = 220, \text{ and } R_{EN}(780 \text{ nm}) = 395$. Some of the variability is caused by
29 changing cloud amounts within the moving region of totality during the 2.7 minutes needed to measure
30 each wavelength channel.

31 Keywords: Atmospheric Processes, Eclipse, DSCOVR/EPIC, Reflected Energy

32 Correspondence email: jay.r.herman@nasa.gov

33 ¹University of Maryland Baltimore County JCET

34 ²Morgan State University, Baltimore Maryland

35 ³NASA Goddard Space Flight Center, Greenbelt, Maryland

36 ⁴Science Systems and Applications, Lanham, Maryland

37 ⁵Goddard Earth Sciences Technology & Research (GESTAR) Columbia, Columbia, MD 21046, USA

38 ⁶SciGlob Instruments and Services, Elkridge, Maryland USA

39 1.0 Introduction

40 Measured radiances of the entire sunlit Earth were obtained during the 21 August 2017 eclipse from
41 EPIC (Earth Polychromatic Imaging Camera) on the DSCOVR (Deep Space Climate Observatory) satellite.
42 DSCOVR obtains synoptic observations of the Earth from an orbit around the L₁ point (Lagrange 1) 1.5
43 million km from Earth (Herman et al., 2018). This study focuses on data from two selected locations
44 during the 21 August 2017 eclipse that crossed the United States from west to east. The locations
45 selected were Casper, Wyoming and Columbia, Missouri, both near the center of the path of totality and
46 both with a nearly overhead total solar eclipse (local time 11:45 in Casper, Wyoming and 13:12 in
47 Columbia, Missouri). The sites were selected in advance to have a high probability of almost cloud-free
48 skies, and so that totality would occur about 30 minutes apart in UTC (Coordinated Universal Time) to
49 accommodate the satellite's ability to acquire data. On the day of the eclipse, Casper, Wyoming had
50 almost clear skies (Fig. 1), with some high thin clouds visible, while Columbia, Missouri had thin low
51 altitude cloud cover (Fig. 2).

52 Observations of total solar eclipses have been made with varying degrees of sophistication for
53 thousands of years as reviewed by Littman et al. (2008). At a given location, observations of reduced
54 irradiance reaching the Earth's surface are limited to just a few minutes of totality and about two hours
55 of partial obscuration (Meeus, 2003). The totality region (umbra) is an oval of about 110 -120 km in size
56 near local noon at Casper, Wyoming and Columbia, Missouri, but will change size and shape as a
57 function of local solar zenith angle (<https://eclipse2017.nasa.gov/eclipse-maps>). Some of the
58 complicating factors concerning quantitative eclipse observations include the effects of the solar corona
59 and light scattered in the atmosphere (Liendo, and Chacin, 2004; Emde and Mayer, 2007).

60 A detailed analysis of an eclipse that occurred in 2006 over southern Europe includes both ground-
61 based and space-based polar orbiting MODIS (Moderate Resolution Imaging Spectroradiometer)
62 observations of cloud cover before totality (Gerasopoulos et al., 2008) as well as theoretical modelling of
63 the eclipse, but unlike the present study, it was largely limited to local effects near the region of totality.
64 A comparison from a meteorological radiation model and measurements of total solar irradiance were
65 made near Athens Greece (84 % of a total eclipse) that showed good agreement in the presence of light
66 clouds (Psiloglou and Kambezidis, 2007). A 3D Monte Carlo radiative transfer study (Emde and Mayer,
67 2007) was applied to the geometry for the nearly overhead total eclipse of 29 March 2006 (13:20 local
68 time in Turkey) to estimate the downward global radiation at the surface, but without the effect of
69 clouds included in the calculation. An application of the 3D model to the 2006 eclipse over Kastelorizo,
70 Greece with fairly cloud-free measurements (few cumulus, 1-2 octas, and scattered cirrus, 3-4 octas) at
71 380 nm showed good agreement for the ratio (ratio = 217) of global surface irradiance starting 5
72 minutes before totality to that during totality (Kazantzidis et al., 2007). Successful modelling of the light
73 levels during an eclipse under realistic conditions is the first step to improved modelling of high cloud
74 reflection and shadowing of solar radiation on the Earth's energy balance.

75 The observations from the DSCOVR satellite are part of a larger project that combines
76 simultaneously obtained satellite and ground-based measurements using a pyranometer (Ji and Tsay,
77 2000) and the Pandora Spectrometer Instrument (Herman et al., 2009) at both sites. The combination

78 will be used to help validate three dimensional (3D) radiative transfer models applicable to analysis of
79 eclipse effects on radiances reflected back to space and reaching the Earth's surface. This study presents
80 the only **calibrated spectral** synoptic satellite data of the sunlit Earth ever obtained during an eclipse,
81 which should place tighter limits on validating radiative transfer studies under realistic conditions. The
82 data includes EPIC measured ozone absorption **(316±5 DU Casper and 305±5 DU for Columbia, see Fig.**
83 **A3)**, O₂ A- and B-band absorption, clouds, aerosols, and scene and surface **reflectivity (Herman et al.,**
84 **2018; Marshak et al., 2018).**

85 DSCOVR observations of the entire sunlit Earth from the eclipse day, 21 August 2017, are compared
86 to those from two non-eclipse days to quantify the change of the global **integral of** reflected solar
87 radiation caused by the eclipse. We present a potential validation test data set for the 21 August 2017
88 eclipse for 3D radiative transfer models, namely the ratio of radiances without the eclipse on 20 and 23
89 August to the same regions that contained totality on 21 August 2017 (based on a suggestion in the
90 paper by Emde and Mayer, 2007).

91

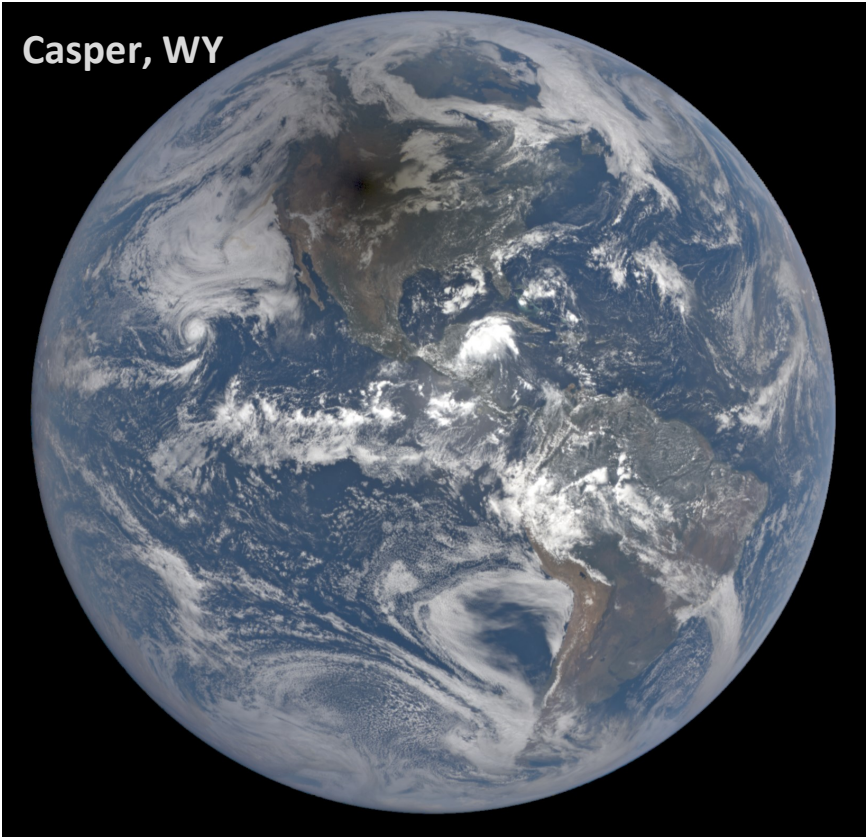


Fig. 1 Synoptic view of the sunlit Earth perturbed by the 21 August 2017 total eclipse centered over Casper, Wyoming at 17:44:50 UTC. The black region is the eclipse umbra centered over Casper, WY. The color image has been adjusted from the images on <https://epic.gsfc.nasa.gov/> by increasing the gamma correction to bring out the region of totality and surrounding clouds.

92



Fig. 02 Synoptic view of the total eclipse centered over Columbia, Missouri at 18:14:50 UTC. The black region is the eclipse umbra centered over Casper, WY. The color image has been adjusted from the images on <https://epic.gsfc.nasa.gov/> by increasing the gamma correction to bring out the region of totality and surrounding clouds.

93

94 Section 2 describes the DSCOVR/EPIC instrument, available data, and monochromatic images based
95 on measured counts per second, C/s. Section 3.1 presents a comparison between eclipse and non-
96 eclipse days. Section 3.2 gives an estimate of the global reduction of reflected sunlight during the eclipse
97 over Casper, WY and Columbia, MO.

98

99 2.0 EPIC Instrument and Data Description

100 The EPIC instrument onboard the DSCOVR spacecraft, in a six-month orbit near the L_1 point
101 since June 2015, observed the Moon's shadow for about 3 hours. The EPIC data comprises a set of seven
102 observations (16:44 to 19:44 UTC) starting in the Pacific Ocean and ending in the Atlantic Ocean, while
103 synoptically observing the entire sunlit disk of the Earth (nominal size 0.5°). EPIC is a 10 wavelength
104 filter camera with a 2048x2048 pixel CCD (charge couple detector) using a 30-cm aperture Cassegrain
105 telescope with a field of view (FOV) of 0.62° that continuously points at the sunlit Earth. The sampling
106 size on the Earth is nominally 8 km at the center of the image with an effective spatial resolution of
107 $10 \times 10 \text{ km}^2$ for the 443 nm channel and $17 \times 17 \text{ km}^2$ for the remaining 9 filter channels. Operation of EPIC
108 consists of sequentially selecting a filter from 2 rotatable filter wheels and an exposure time using a
109 rotating disk shutter mechanism. Invariant exposure times were set at the beginning of the on-orbit

110 mission to fill the CCD wells to about 80 % and avoid blooming (a saturated pixel affecting its neighbors).
111 The CCD was calibrated for the sensitivity differences between the pixels (flatfielding), and
112 measurements were made in the laboratory and in-flight to obtain corrections for stray light effects.
113 Corrections for dark current are applied based on periodic measurements with the shutter closed. EPIC
114 is kept centered on the Earth during its 6-month north-south tilted Lissajous orbit about the Earth-Sun L_1
115 point. The spacecraft is never closer than 4° from the Earth-Sun line, which makes it possible to observe
116 an eclipse without the Moon being in the FOV. On 21 August 2017, DSCOVR was 7.7° from the Earth-Sun
117 line. A more detailed description of EPIC is given in Herman et al. (2018) and Marshak et al., (2018).

118 The geolocated EPIC data (Counts per second, C/s) from each set of 10 wavelengths are
119 contained in an HDF5 formatted file available from the permanent NASA Langley data repository center
120 (https://eosweb.larc.nasa.gov/project/dscovr/dscovr_epic_l1b). Contained in each Level-2 data HDF5
121 file are the 2048 x 2048 array of C/s measured by EPIC and a common latitude and longitude grid. The
122 geolocated data are organized corresponding to the rectangular CCD grid, 1 data point per CCD pixel.
123 For the time of the eclipse, the illuminated CCD pixels are within a circular boundary corresponding to
124 $N_p = 2.59 \times 10^6$ illuminated pixels (illuminated pixels formed a circle of 1816 pixels in diameter out of a
125 maximum of 2048 pixels. To reduce the volume of telemetry data, all measurements, except those from
126 the 443 nm channel, were 2×2 averaged onboard DSCOVR to 1024 x 1024 pixels. After geolocation onto
127 a common latitude x longitude grid, the data from all channels are presented as 2048 x 2048 points with
128 off-earth points represented as a fill value "infinity". All of the data products (e.g., ozone amounts) are
129 also available at the above repository center.

130 The EPIC file names from the NASA data repository are interpreted as Year 2017, Month 08, Day
131 21, UTC 17:44:50, Version 2, which is 11:44:50 local daylight savings time in Casper, Wyoming. The
132 filename time refers to approximately the middle of the measurement sequence. Totality in Casper
133 started at 11:42:39 and ended at 11:45:05. Version 2 refers to the reprocessing of data with the latest
134 CCD flat-fielding and stray-light corrections (Herman et al., 2017; Marshak et al., 2017; Geogdzhayev and
135 Marshak, 2017), and the geolocation algorithms.

136 The observing conditions for 21 August 2017 ranged from significant cloud cover over the oceans to
137 nearly clear skies over the United States (Figs. 1 and 2). The synoptic observations provided a unique
138 opportunity to estimate the fraction of reduced reflected radiation from the entire sunlit Earth caused
139 by a total solar eclipse. Two of the synoptic observations were timed so that they centered on Casper,
140 Wyoming (42.8666° N, 106.3131° W, 17:44:50 UTC) and Columbia, Missouri (38.9517° N, 92.3341° W,
141 18:14:50 UTC). Ten narrowband images were obtained at center vacuum wavelengths λ_i of 317.5 ± 0.5 ,
142 325 ± 0.5 , 340 ± 1.3 , 388 ± 1.3 , 443 ± 1.3 , 551 ± 1.5 , 680 ± 0.8 , 688 ± 0.42 , 764 ± 0.5 and 779.5 ± 0.9 nm (Herman
143 et al., 2018). Of these, 388, 443, 552, 680, and 779 nm radiances are not strongly absorbed in the
144 atmosphere and are used for estimating the reduction in reflected radiances from the Earth. The others
145 are strongly affected either by ozone (317, 325, 340 nm) or oxygen absorption (688, 764 nm) in the
146 atmosphere, but give similar radiance percent reductions during the eclipse compared to non-absorbed
147 channels.

148 The non-absorbed wavelength observations were combined to produce eye-realistic color images
 149 (<https://epic.gsfc.nasa.gov>). For this eclipse day study, 21 August, the original color images were
 150 modified by increasing the gamma correction to better show the umbra over Casper, Wyoming and
 151 Columbia, Missouri (Figs. 1 and 2 based on a suggestion by Steven Albers and Michael Boccara, 2017,
 152 Private Communication). The images include Rayleigh scattering effects that cause light from the
 153 penumbral region to increase illumination within the umbra along with scattering from clouds and
 154 aerosols.

155 Table 1 summarizes eclipse timing and location details for Casper, Wyoming. During the 2.7
 156 minutes needed to obtain the five listed wavelength channel images, the center of totality moves at
 157 about 46 km/minute or covering approximately 124 km. Based on the image in Fig. 1, the entire
 158 measurement took place within the observed nearly clear-sky region surrounding Casper, Wyoming. **A**
 159 **similar table could be constructed for the eclipse totality region near Columbia, Missouri.**

Table 1 *Eclipse Measurement Timing and Location Details for 5 Wavelengths*
 Eclipse Maximum and EPIC Image Times. Total Measurement Duration 2.7 minutes

Wavelength (nm)	Date and Time	Location Name	Longitude
	2017-08-21 17:35:40	Eclipse West Edge of WY state	-111 ⁰ 02'
551	2017-08-21 17:42:36	West of Casper	-106 ⁰ 22'
680	2017-08-21 17:43:30	West of Casper	-106 ⁰ 21'
Casper Wyoming	2017-08-21 17:43:51	Casper WY	-106 ⁰ 19'
780	2017-08-21 17:44:24	Near Glenrock WY	-105 ⁰ 52'
443	2017-08-21 17:44:50	West of Douglas WY	-105 ⁰ 14'
388	2017-08-21 17:45:18	West of Douglas WY	-105 ⁰ 17'
	2017-08-21 17:48:04	Eclipse East Edge of WY state	-104 ⁰ 03'

160
 161 The timing and predicted shape of the Moon's shadow over Casper, Wyoming **and Columbia,**
 162 **Missouri** can be seen at <https://eclipse2017.nasa.gov/eclipse-maps>. An annotated portion of the figures
 163 for Casper **and Columbia are** reproduced in the Appendix (Fig. A1). The predicted totality shadow (Fig.
 164 A1) over Casper was elliptical in shape with a width of about 116 km (about 1.5⁰ in latitude or
 165 longitude). The similar drawing for Columbia, Missouri shows a more nearly circular region of totality.
 166 The dimension of the partial eclipse for 90 % obscuration is about 5⁰ in latitude or longitude. **The region**
 167 **of 75 % obscuration covers a latitude range 32⁰ to 46⁰ or about 1200 km.** An obscuration region of this
 168 size produces a significant decrease in the percentage of total solar irradiance reaching the Earth's
 169 surface and in the amount reflected back to space. EPIC synoptically measures both the local and sunlit
 170 portion of the global percent change in reflected radiance, which is approximately the same as the
 171 percent change in **global** surface irradiance for the wavelength range from 388 to 780 nm. **An exception**
 172 **is within the umbral region, where the percent change is larger at the surface than at the top of the**
 173 **atmosphere.** **The three wavelength channels shorter than 388 nm are affected by ozone absorption and**
 174 **also do not contribute much to the sum of reflected radiances compared to the range from 388 to 780**
 175 **nm. The energy content of 317 to 340 nm are not included in the quantitative estimate of broadband**
 176 **(UV + visible) reduced reflected radiance, nor are the strongly absorbed O₂ A- and B-band channels, 688**
 177 **and 764 nm, included. However, the effects of the eclipse on all 10 channels are individually estimated.**
 178

179 **2.1 Monochromatic Eclipse Images**

180

181 Before quantitatively examining the EPIC data from the eclipse in units of C/s or reflectance, the
182 same data can be represented as monochrome grey-scale images. The images (Fig. 3 with North down)
183 range from 340 nm, with strong Rayleigh scattering effects and some ozone absorption, to 780 nm in
184 the near infrared. North is selected as down to correspond to a 3D projection image presented later.
185 Because of the clarity of the atmosphere at 780 nm, the image serves as a geographic map of the Earth
186 as viewed by EPIC where North and South America are clearly visible.

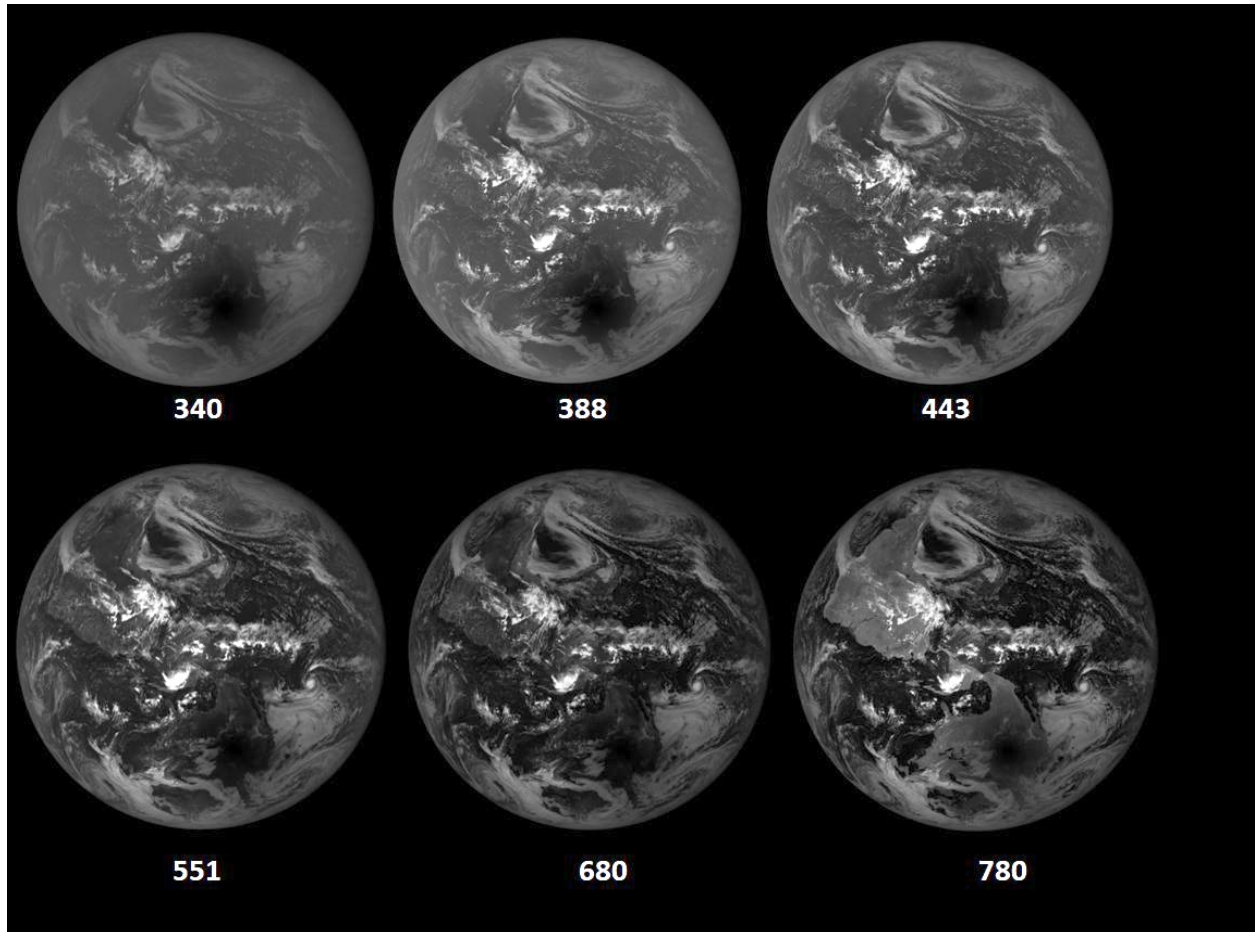


Fig. 3 Greyscale images for 6 of the DSCOVR/EPIC channels for the eclipse over Casper Wyoming showing the blurring caused by Rayleigh scattering and the dark land and ocean surfaces at 340 nm to the almost clear atmosphere and bright continental surfaces at 780 nm. The images were obtained over a period of 2.7 minutes. North is facing down.

187

188

189

190

191 **3.0 Results**

192 **3.1 Comparison of EPIC Observations of Eclipse Totality (21 Aug) with Non-Eclipse Days (20 and 23**
193 **Aug) for Casper, WY and Columbia, MO**

194 Atmospheric conditions during the eclipse at Casper, Wyoming were almost cloud-free
195 compared to Columbia, Missouri, which had optically thin low altitude clouds (Fig. 2). Figure 4 shows the
196 cloud cover on the day of the eclipse, 21 August 2017 (panel A) about 90 minutes before totality at
197 Casper and about 2 hours after totality. The images (north is up) show that the skies remained relatively
198 clear over the northern United States for the duration of the eclipse. A similar set of images (panel B)
199 are shown for the day before (20 August) and two days after the eclipse (23 August). There was no
200 useable data available on 22 August. Data obtained on 20 and 23 Aug. at approximately the same UTC
201 (backscatter phase angle for a given location on Earth) as occurred during the total eclipse are used as
202 reference data to compare with the eclipse data on 21 Aug. The basic global patterns of cloud cover are
203 similar for all three days, but not identical. As shown later, the amount of light reflected back to space is
204 approximately the same on the two non-eclipse days 20 August and 23 August.

205

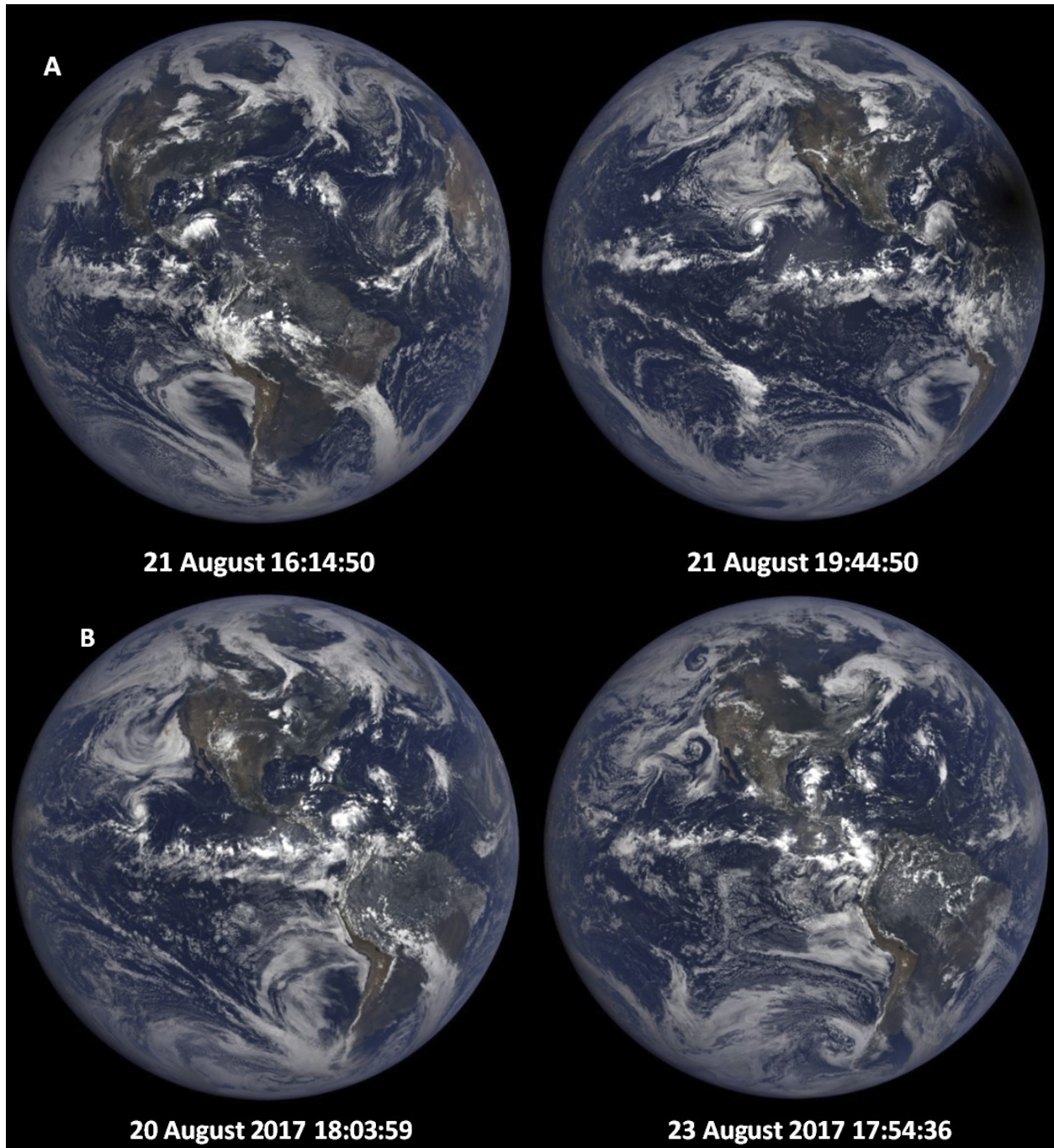


Fig. 4 Panel A: Synoptic natural color images on 21 August at 16:14 and 19:44 before and after the eclipse over the US, and Panel B: the days before and after the eclipse selected to be as close as possible to the phase angle (UTC 17:44:50) as the time of totality over Casper, Wyoming. North is facing up.

206

207 Figure 5 (upper panels A and B) shows longitudinal slices of 443 nm reflected solar radiances in
 208 C/s towards L_1 through the locations corresponding to Casper, Wyoming and Columbia, Missouri at their
 209 respective times of totality. The lower panels (C and D) of Fig. 5 show 443 nm measurements in C/s on
 210 20 Aug at 18:04 UTC before the eclipse for nearly identical solar phase angles conditions for both sites.

211 The effect of clouds at the Columbia site compared to Casper can be seen in terms of the depth of the
 212 umbra (Panels A: ratio = 1530 and B: ratio = 37) relative to the average C/s from -140° to -150°
 213 longitude. Similarly, on the preceding day, 20 Aug (panels C and D), the cloud effect is small at Casper,
 214 1.2×10^4 C/s, compared to Columbia, 5×10^4 C/s and just to the west of Columbia, 1.3×10^5 C/s.
 215

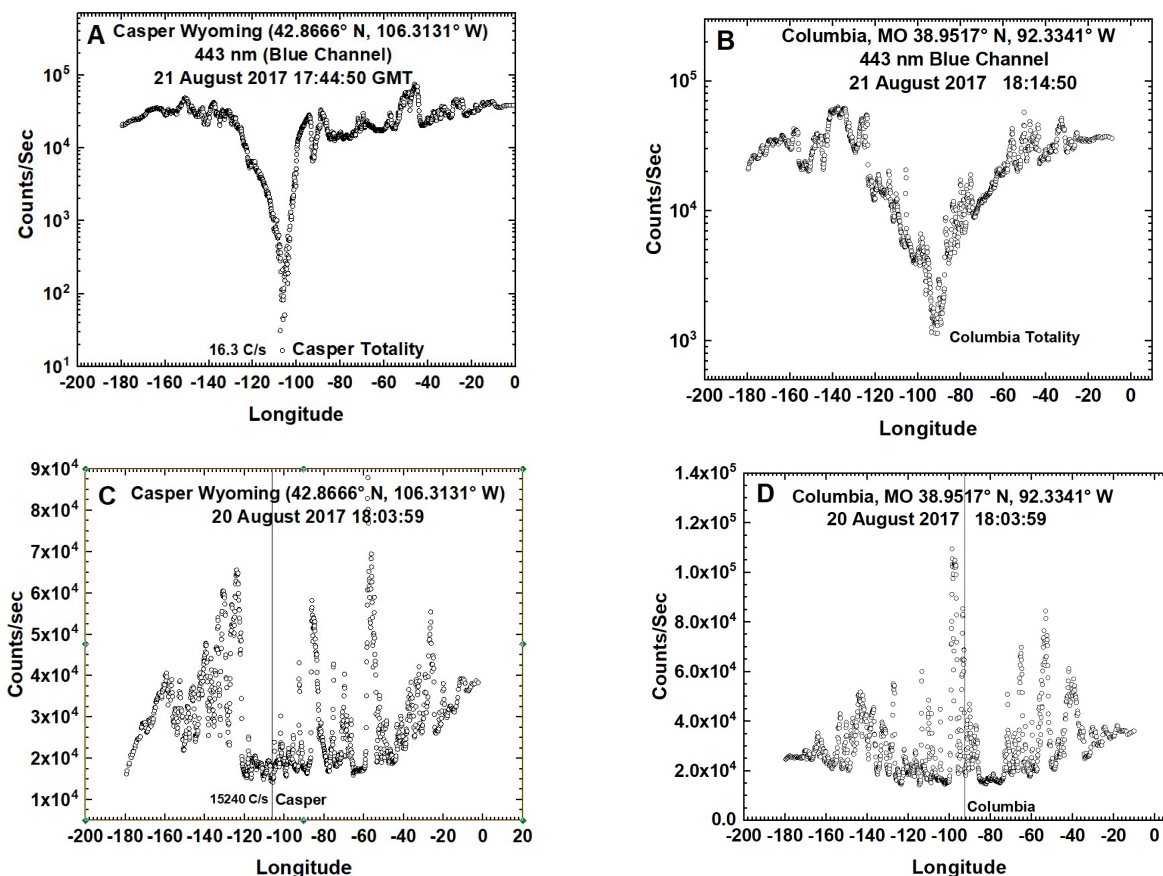


Fig. 5 Top: The effect of an eclipse (21 Aug) on the measured C/s reflected back to space as a function of longitude (degrees) for two locations, Casper Wyoming (left) and Columbia Missouri (right). Bottom: Measured C/s reflected back to space on 20 Aug. A log₁₀ scale is used to show details of the spatial variability mostly caused by clouds.

216
 217 The minimum 443 nm values during totality are 16.6 C/s for Casper and 312 C/s for Columbia.
 218 On 20 Aug. EPIC measured 15240 C/s and 52728 C/s, respectively, showing the effect of increased
 219 cloudiness for Columbia. While Fig. 5 is expressed in C/s, the data can be converted to radiance $W/(m^2$
 220 $nm\ sr)$ based on an in-flight determined radiance calibration coefficient of $K_R(443nm) = 5.291 \times 10^{-6}$
 221 $W/(m^2\ nm\ sr\ C/s)$ (Geogdzhayev and Marshak, 2017; Marshak et al., 2018; Herman et al. 2018). For 443
 222 nm channel, an average count rate for the illuminated earth is 3×10^4 C/s corresponding to a radiance of
 223 $0.159\ W/(m^2\ nm\ sr)$. EPIC calibration constants for 8 of the 10 channels were obtained by in-flight
 224 comparisons of reflectance measured by two well calibrated low Earth orbiting satellite instruments,
 225 OMPS (Ozone Mapping Profiler Suite for UV channels) and MODIS (Moderate Resolution Imaging
 226 Spectroradiometer for visible and near-IR channels) for simultaneously viewed Earth areas with the

227 same satellite view and solar zenith angles (Herman et al., 2018; Geogdzhayev and Marshak, 2017). The
 228 O₂ A- and B-band channels were calibrated using lunar data when the Moon was within the field of view
 229 of EPIC. Detailed discussions and values of all EPIC calibration coefficients $K(\lambda)$ are given by Geogdzhayev
 230 and Marshak (2017), Herman et al, (2018) and Marshak et al., (2018). Most of the conclusions in this
 231 study are in terms of ratios of C/s from the same wavelength channel at approximately the same solar
 232 phase angle that are independent of the absolute calibration conversion from C/s to radiance.

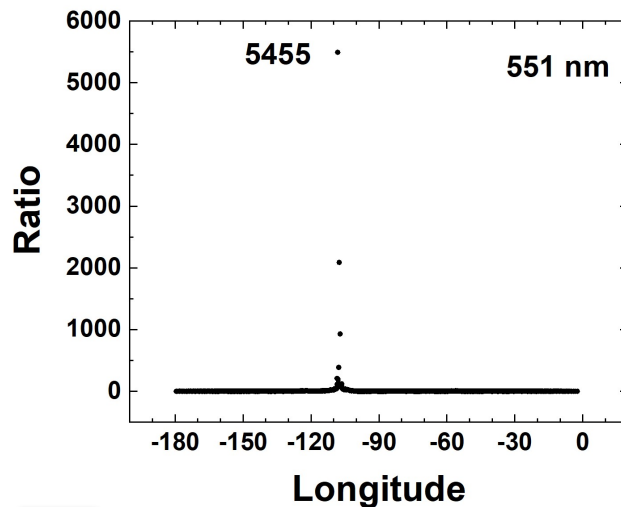
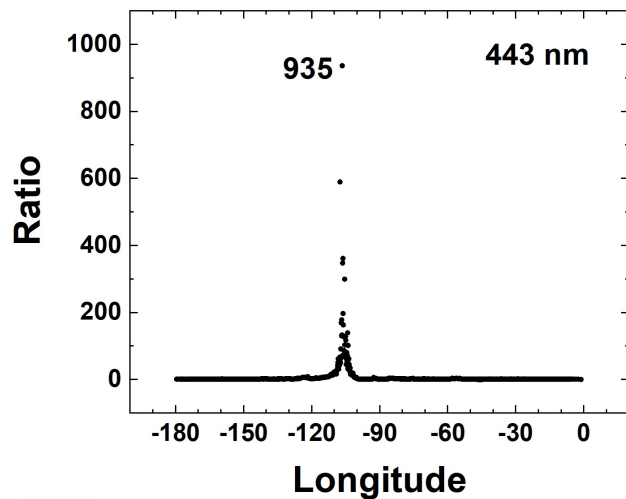
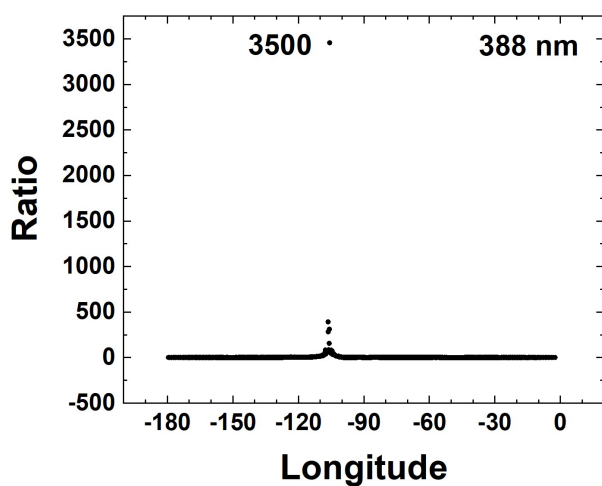
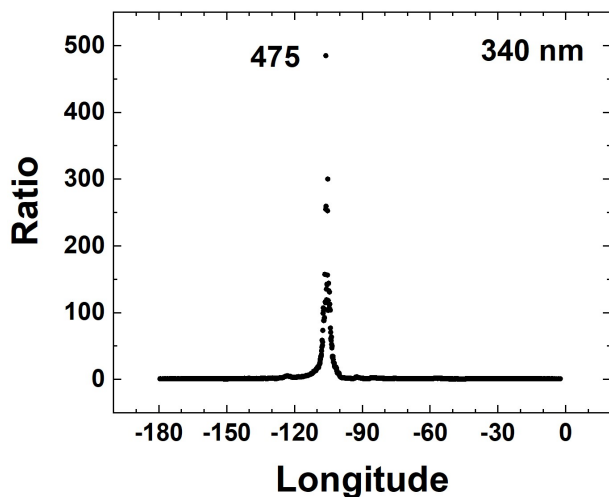
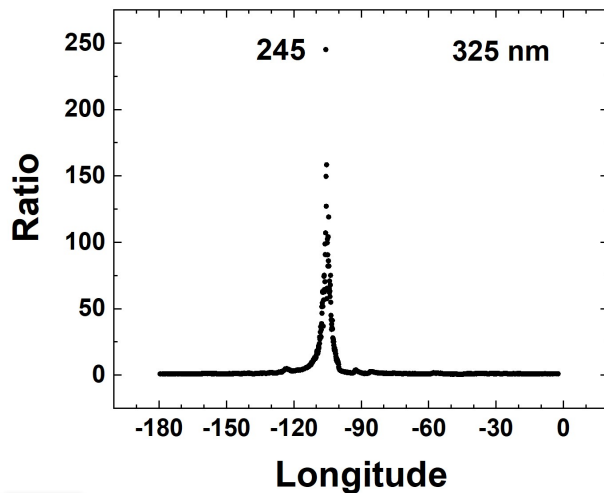
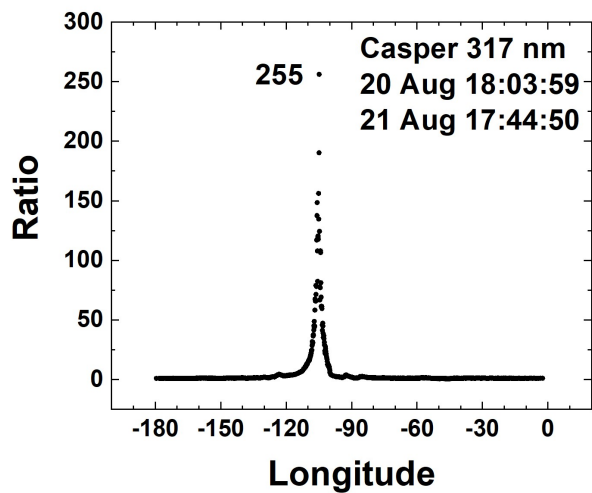
233
 234 The ratio $R_{EN}(\lambda_i) = I(20 \text{ August})/I(21 \text{ August})$ is used to characterize the eclipse effects at the top
 235 of the atmosphere. Because the solar phase angles are nearly the same, the effects of the 172°
 236 backscatter angle (“hot spot” caused mostly by minimized shadows) and ocean specular reflection are
 237 also nearly the same on both days.

238 There is considerable variability in $R_{EN}(\lambda_i) = I(20 \text{ August})/I(21 \text{ August})$ as a function of wavelength
 239 that is partially caused by the 2.7 minutes needed to obtain measurements for all 10 wavelengths.
 240 During the 2.7 minutes, the center of totality moved about 124 km or about 1.7° longitude, meaning
 241 that the ratio was affected by atmospheric variability (mostly cloud effects) in the successive scenes
 242 containing the eclipse totality for each wavelength. The ratios $R_{EN}(\lambda_i)$ of C/s on the eclipse day to the
 243 preceding non-eclipse day are shown in Fig. 6 for all 10 wavelength λ_i channels and two sites (Casper, Fig
 244 6a and Columbia, Fig. 6b) and summarized in Table 2. The same reference data from 20 Aug is used for
 245 both sites, since it was the closest in UTC for both the Casper and Columbia eclipse times.

246

247 *Table 2 Maximum Radiance Ratio $R_{EN}(\lambda_i)$ during eclipse totality 17:44:50*
 248 *UTC (Casper) and 18:14:50 UTC (Columbia) compared to 20 Aug. at*
18:03:59 for both sites (see Fig. 6).

Wavelength λ_i (nm)	Max. $R_{EN}(\lambda_i)$ C/s	Max. $R_{EN}(\lambda_i)$ C/s
	Casper, Wyoming	Columbia, Missouri
317.5	255	50
325	245	49
340	475	59
388	3500	81
443	935	169
551	5455	183
680	220	171
688	365	246
764	302	92
780	395	38



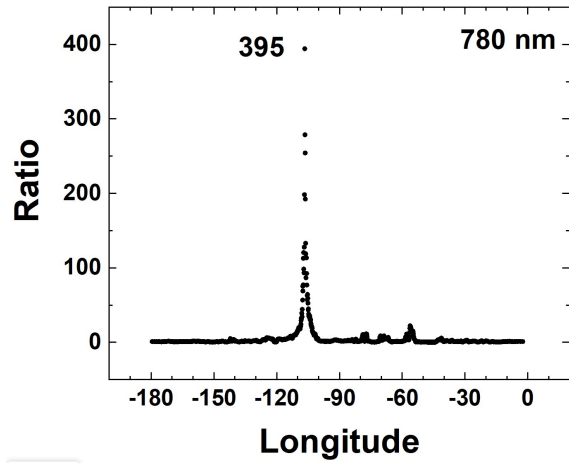
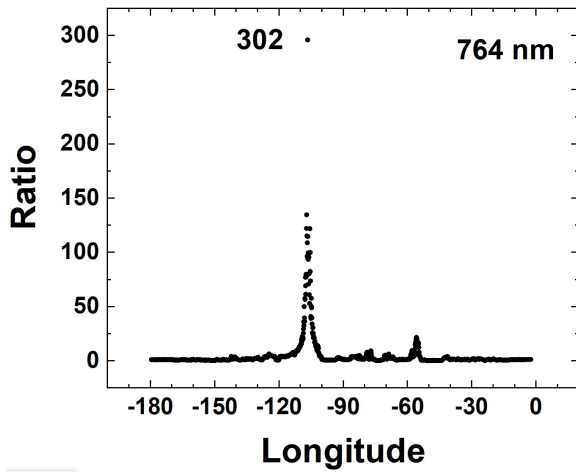
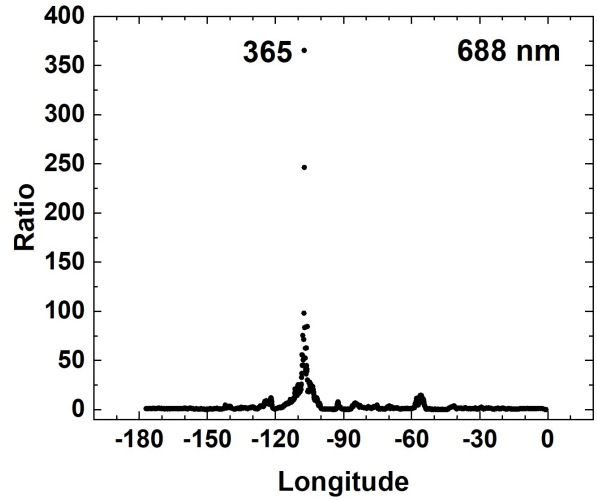
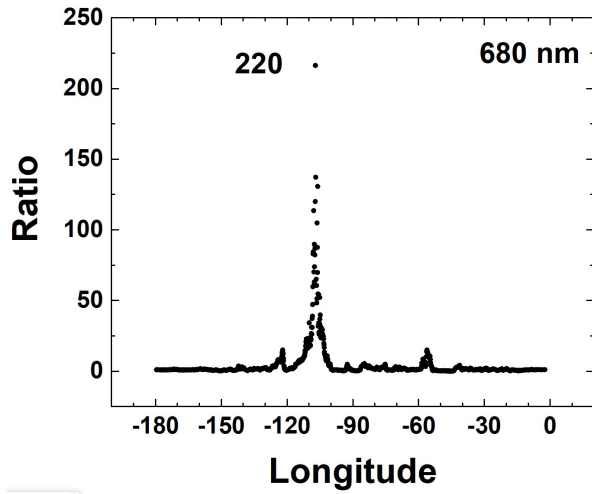
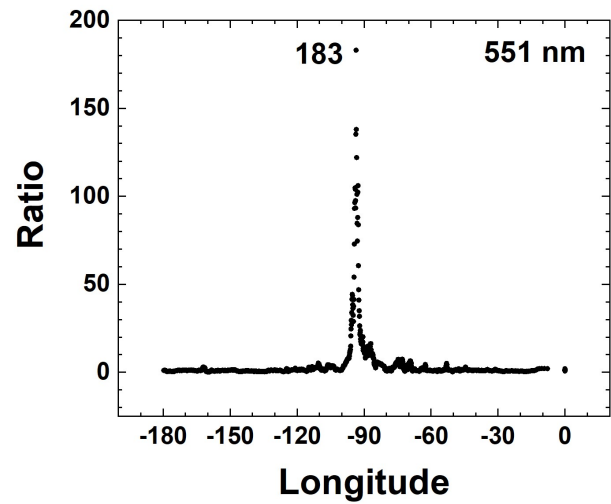
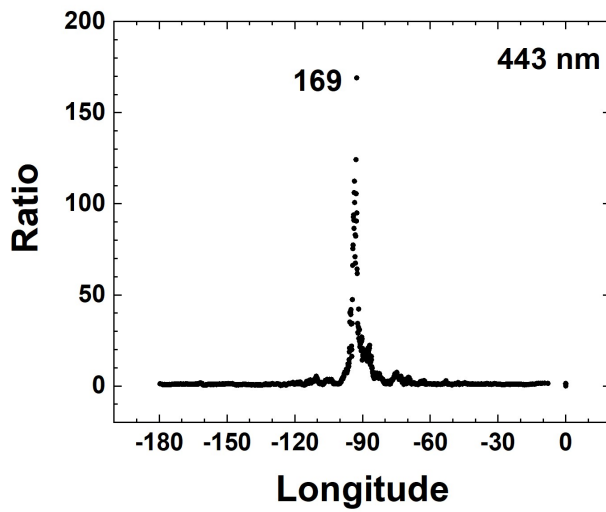
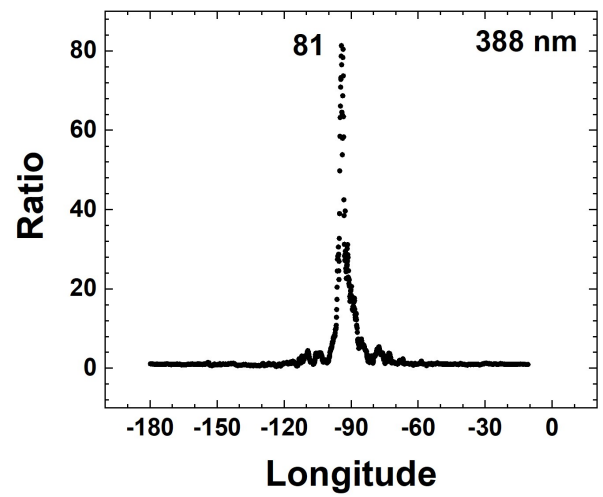
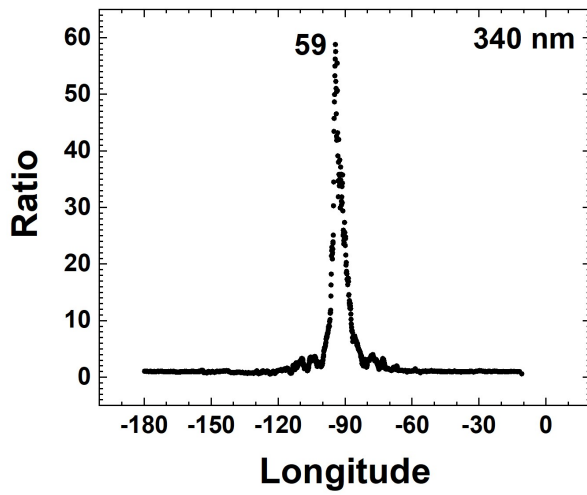
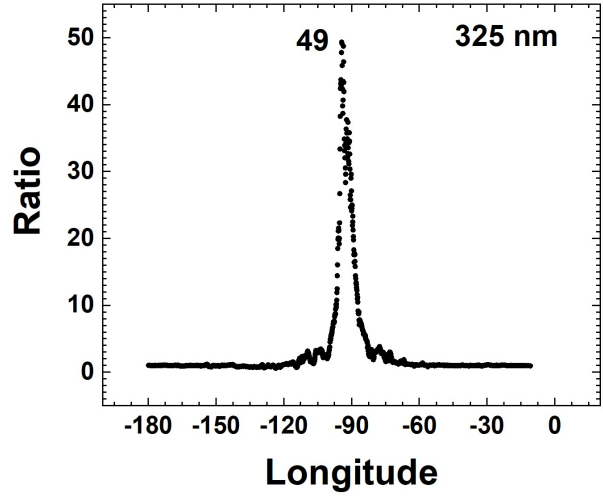
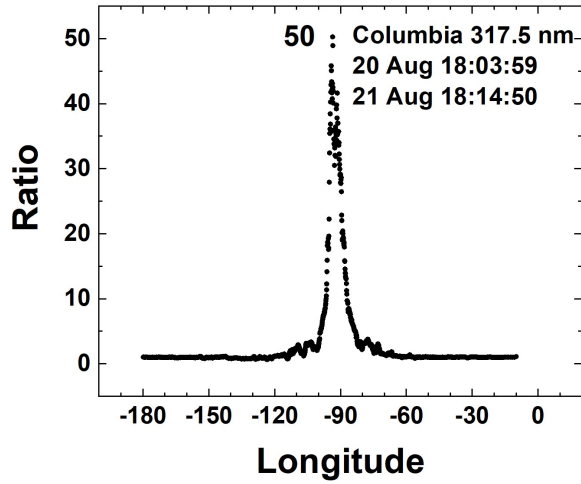


Fig. 6a. The ratio $R_{EN}(\lambda_i) = I(\text{Aug20})/I(\text{Aug21})$ at the time of the Eclipse in Casper Wyoming for wavelengths 317.5 to 780 nm. The channels 317.5 to 240 nm are affected by ozone absorption and the channels 688 and 764 nm are within the O_2 B and A absorption bands.

252

253



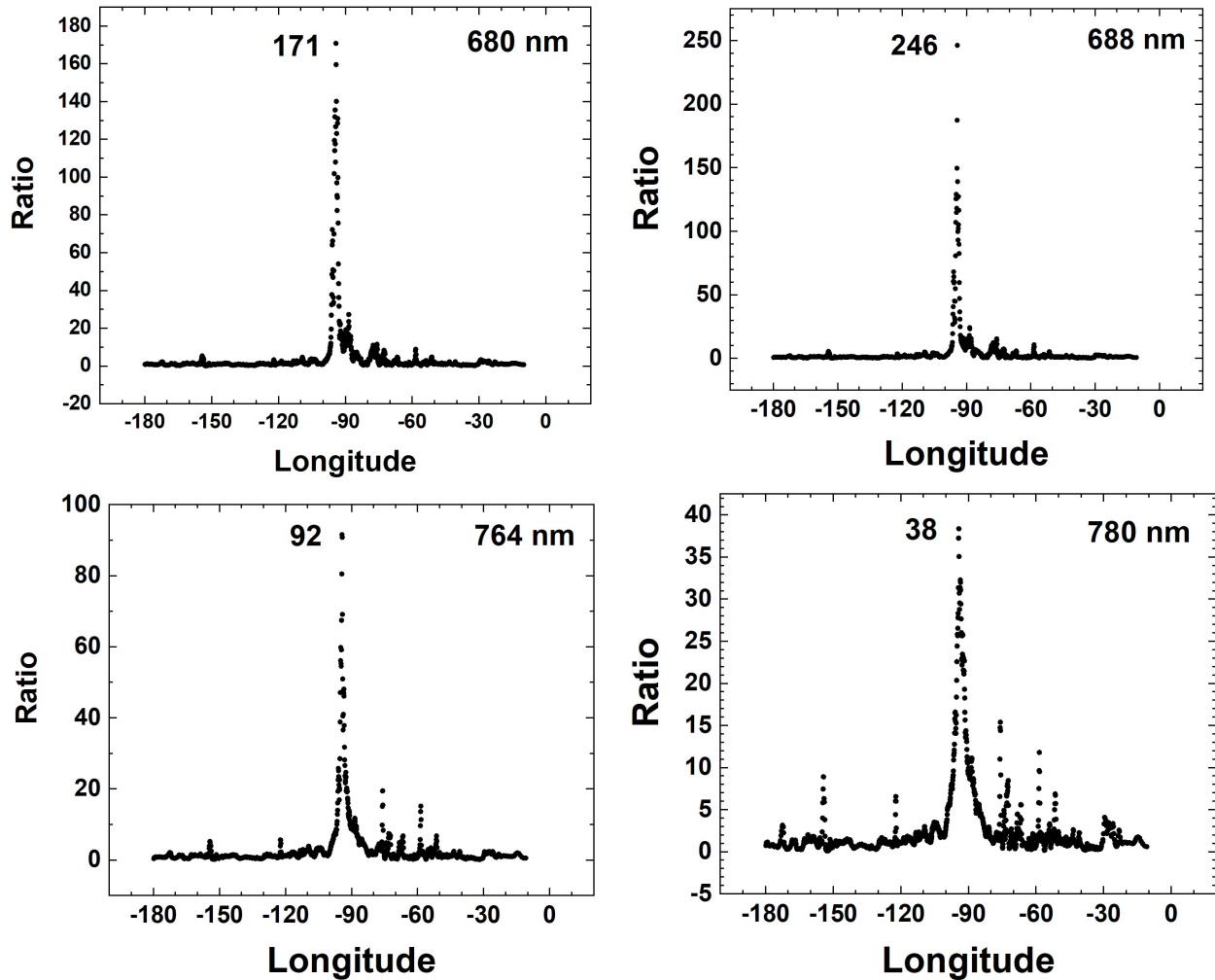


Fig. 6b. The ratio $R_{EN}(\lambda_i) = I(\text{Aug20})/I(\text{Aug21})$ at the time of the Eclipse in Columbia, Missouri for wavelengths 317.5 to 780 nm. The channels 317.5 to 340 nm are affected by ozone absorption and the channels 688 and 764 nm are within the O_2 B and A absorption bands.

255

256 For the eclipse study, the range of synoptically observed longitudes is approximately from the
 257 international dateline (-180°) to almost longitude of Greenwich, England (0°). The nearly clear-sky in
 258 Casper with optically thin high cirrus clouds permits the reflected light during totality to become very
 259 small (about 17 C/s for 443 nm compared to 1.5×10^4 C/s on 20 August at the same longitude). Columbia
 260 had more low altitude cloud cover than Casper (Fig. 2) with the cloud cover extending into the region of
 261 totality. The effect of this cloud cover can be seen in Fig. 6, where the maximum $R_{EN}(443, \text{Columbia}) =$
 262 169 compared to 935 for Casper. Table 2 provides the eclipse radiance ratio $R_{EN}(\lambda_i)$ for the five non-
 263 absorbed wavelength and 5-absorbed channels that can help validate 3D radiative transfer models. The
 264 measured lower values $R_{EN}(\lambda_i)$ at Columbia compared to Casper show that there is high sensitivity in the
 265 TOA upwelling measured ratios to the presence of even optically thin clouds. A detailed radiative
 266 transfer study for realistic conditions is made feasible by using EPIC's simultaneous estimates of cloud
 267 reflectivity and transmission, cloud height, ozone amounts, (Fig. A3 and Herman et al., 2018), and

268 aerosol amounts (Torres et al., 2018 private communication). These data products are available from
269 the NASA-Langley data repository referenced above.

270

271 3.2 Global reduction of reflected sunlight during the eclipse over Casper WY

272

273 The unique DSCOVR/EPIC measurements provide estimates of the fractional reduction of
274 sunlight from 388 to 780 nm reflected back to space for the entire sunlit globe caused by the eclipse
275 shadow on the Earth. To do this, all of the light reaching EPIC in each of the five non-absorbed channels,
276 388, 443, 551, 680, and 780 nm, are integrated over the visible sunlit Earth and compared (percent
277 difference $PD(\lambda_i)$) with a nearly identical viewing geometry (nearly the same UTC) from the previous and
278 next days. The assumption is that the major cloud features change slowly on a global scale over
279 relatively short periods (Figs. 1 to 3). A test of this hypothesis is that the PD between successive non-
280 eclipse days is small compared to the eclipse day $PD(\lambda_i)$ with a non-eclipse day.

281 In the 3D Fig. 7 for 443 nm, the nearly cloud free eclipse region is the blue area in the midst of
282 greens, yellows, and reds. The high red values correspond to fairly reflective clouds mostly seen near
283 the equator (Fig. 1). The yellows and greens correspond to lower altitude clouds that tend to have
284 smaller reflectivities. Integrating over all of the pixels for the eclipse on 21 August 2017, using the file
285 named epic_1b_20170821174450_02.h5, we get $S(\text{DOY}, \text{UTC}) = 5.34366 \times 10^{10}$ C/s for DOY=233 (21
286 August 2017) and UTC=17:44:50. For the eclipse day, the 443 nm average C/s = 2.0631×10^4 , which
287 corresponds to $2.0631 \times 10^4 K_R(443 \text{ nm}) = 0.11 \text{ W}/(\text{m}^2 \text{ nm sr})$. Peak values are approximately 1×10^5 C/s,
288 or about $0.53 \text{ W}/(\text{m}^2 \text{ nm sr})$. Figure 7 is oriented with north down so as to be able to see into the eclipse
289 shadow region. A similar figure is obtained for Columbia, Missouri with reduced depth caused by some
290 visible light cloud cover extending into the region of totality.

291

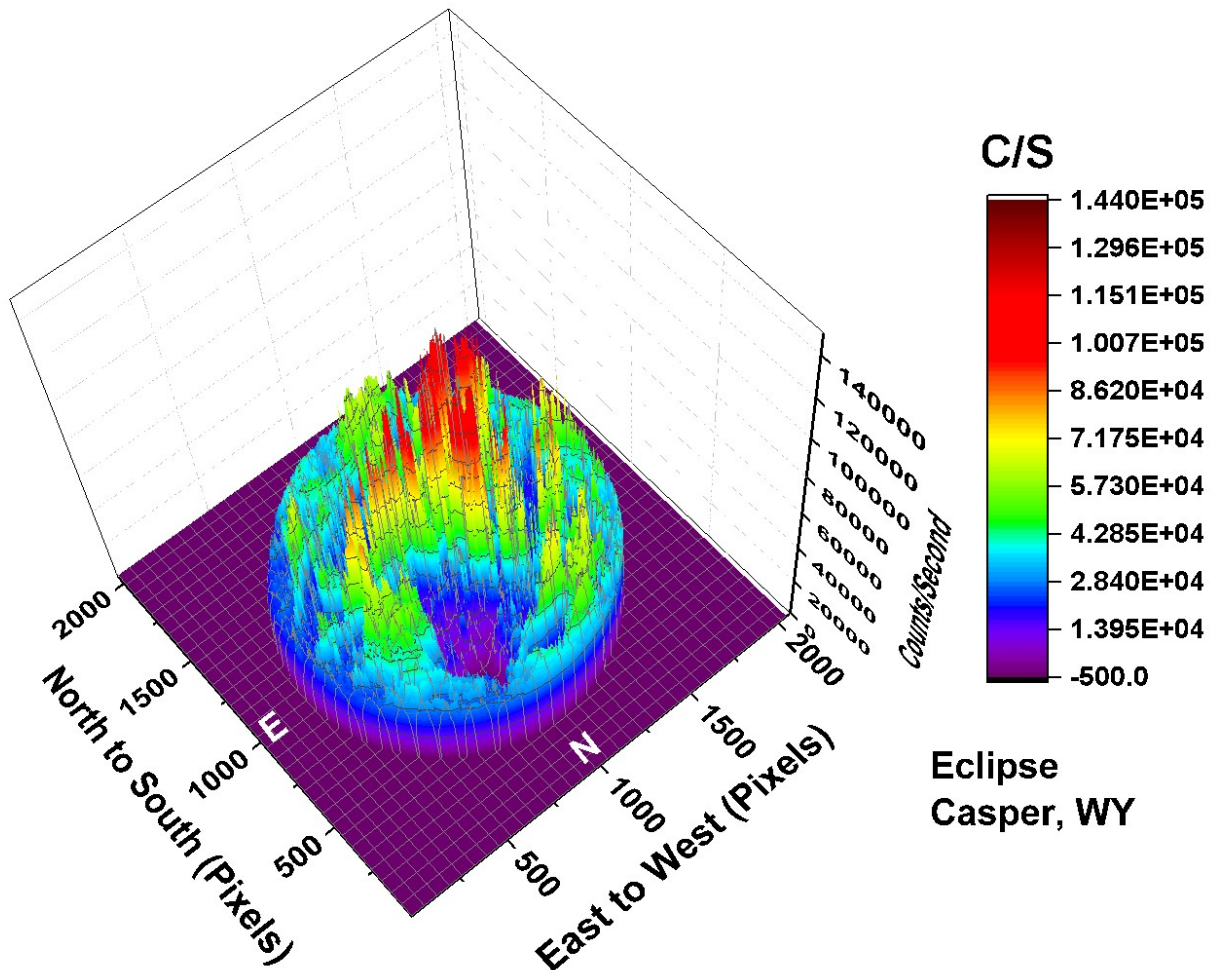


Fig. 7 The C/s observed by EPIC for the 443 nm channel corresponding to the color image shown in Fig. 1. In the data file, the fill-word infinity has been replaced by the number zero. In this image there are approximately $N_p = 2.59 \times 10^6$ illuminated pixels out of $2048^2 = 4.194304 \times 10^6$ pixels (61.8 %).

292

293 Measured C/s images for six wavelength channels (340 to 780 nm) on 20, 21, and 23 August (Fig.
 294 8) were selected to be as close as possible to the UTC time of the eclipse in Casper Wyoming, keeping
 295 the scattering phase angles nearly constant. Similar images for the strongly absorbed channels 317.5,
 296 325, 688, 764 nm channels are shown in the appendix (Fig. A2). The middle images in panels B and E of
 297 Figs. 8a, 8b and 8c are for the eclipse over Casper, Wyoming. These images are in the same format as
 298 Fig. 3, but rotated with north up. Unlike Fig. 3, The scale in Fig. 8 was selected so that the brightest
 299 clouds do not saturate the image. The increase in scale makes the land surfaces less visible. While the
 300 figures are similar from wavelength to wavelength, there are differences in the depth of the eclipse
 301 totality and the reflectivities of the surrounding clouds. In general, the equatorial clouds with higher C/s
 302 (reflectivities) tend to reach higher altitudes. This is confirmed by examining the C/s in the strongly
 303 absorbed O₂ A-band channel (Fig. A2b and Herman et al., 2018).

304

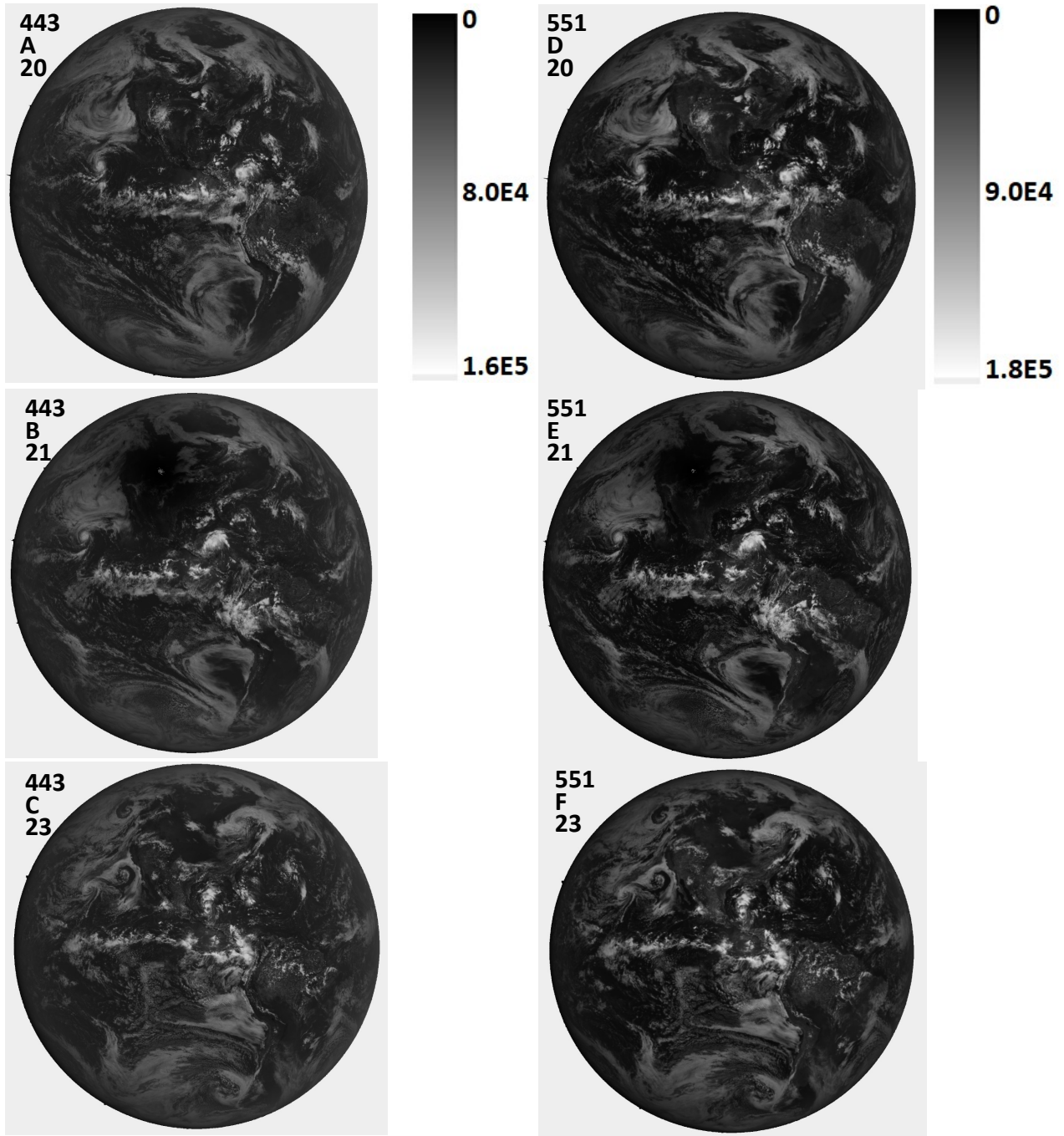


Figure 8a Image in C/s for 443 and 551 nm for 20 Aug. (A+C), 21 Aug. (B+E), and 23 Aug. (C+F). The scale applies to the specific wavelength. North is up.

305

306

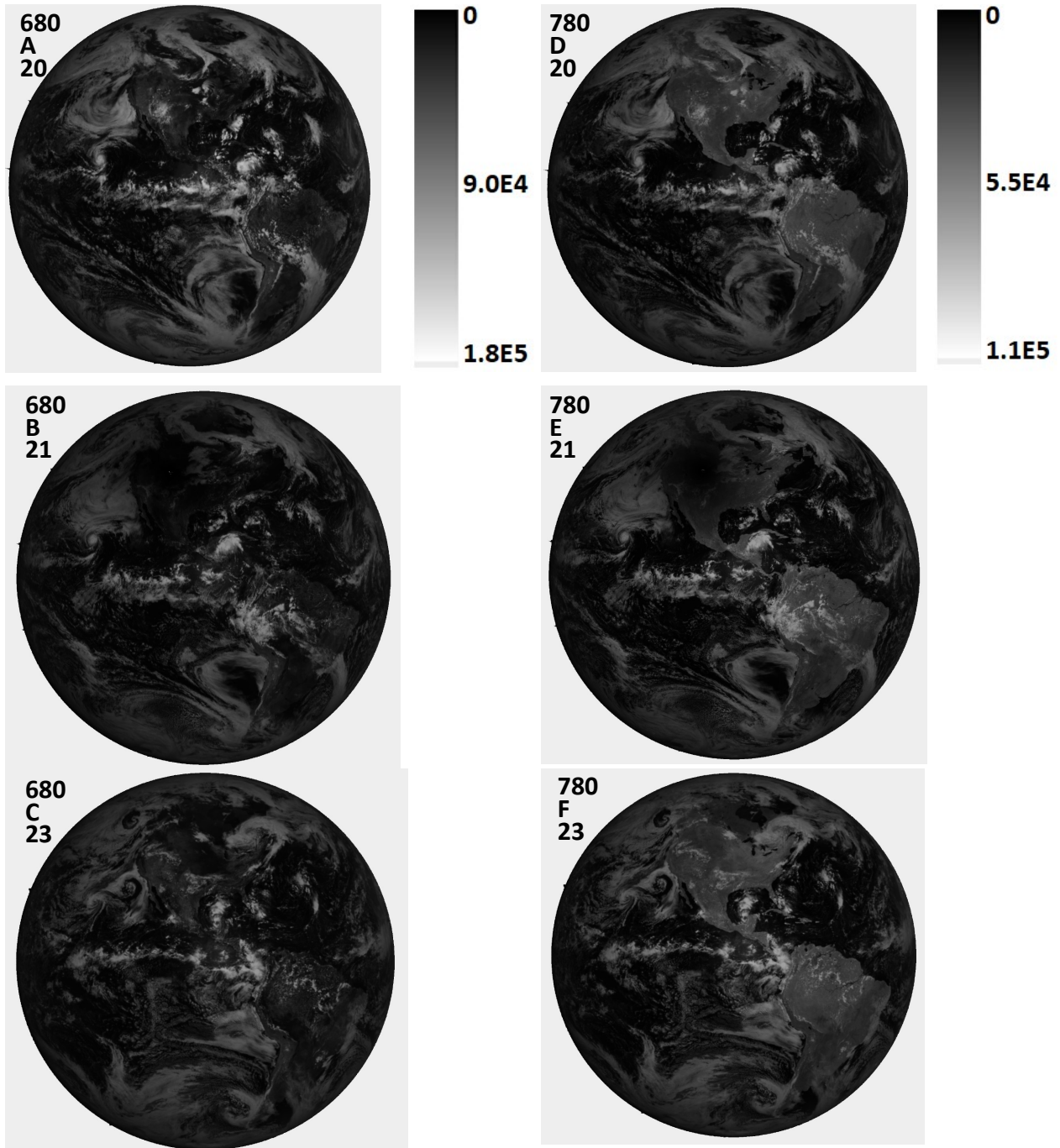


Figure 8b Image in C/s for 680 and 780 nm for 20 Aug.(A+C), 21 Aug. (B+E), and 23 Aug. (C+F). The scale applies to the specific wavelength. North is up.

307

308 EPIC measured $C(\lambda)$ in C/s for each pixel can be converted to Earth top of the atmosphere
 309 reflectance $Re(\lambda)$ using the in-flight derived calibration coefficients $K(\lambda)$, where $Re(\lambda) = K(\lambda) C(\lambda)$. For
 310 the six wavelength channels in Fig. 8 plus the O_2 A- and B-band channels, $K(340) = 1.975 \times 10^{-05}$, $K(388) =$
 311 2.685×10^{-05} , $K(443) = 8.340 \times 10^{-06}$, $K(551) = 6.66 \times 10^{-06}$, $K(680) = 9.30 \times 10^{-06}$, $K(687.75) = 2.02 \times 10^{-05}$, $K(764)$
 312 $= 2.36 \times 10^{-05}$, and $K(780) = 1.435 \times 10^{-05}$ (Herman et al., 2018; Geogdzhayev and Marshak, 2018; Marshak

313 et al., 2018). To estimate the percent reduction in outgoing radiances, the ratios of integrals over the
 314 illuminated CCD for each wavelength channel are formed for nearly the same Earth geometry on days
 315 preceding and following the eclipse. Either the integrated reflectances or the integrated $C/s \times 10^{-7}$ (Eqn.
 316 1) for Tables 3A for Casper, Wyoming and 3B for Columbia Missouri) over the CCD pixels, $ICs(\lambda)$, can be
 317 used directly, since they are linearly proportional to the integral of the photons received by the
 318 illuminated pixels.

319
 320 Table 3 and Fig. 9 show that the global reduction of backscattered light caused by the eclipse is
 321 similar for the two sites even though there is more cloud cover locally over Columbia than Casper. This is
 322 because only 30 minutes have elapsed between the two measurements, which is not enough time for
 323 the global cloud cover to have significantly changed.

324

Table 3A Global integral of reflected light ICs for the UTC of the Casper, WY eclipse on 21 August and for the closest solar phase angle from 20 and 23 August. PD is the percent difference caused by the eclipse. Units are $ICs \times 10^{-7}$

λ_i (nm)	20 August 2017 16:58:31 UTC	21 August 2017 17:44:50	23 August 2017 17:54:36	Avg. PD
317.5	280.5	258.8	282.0	9±0.3
325	460.6	425.5	464.2	9±0.4
340	3183	2946	3213	9±0.5
388	2034	1878	2044	9±0.3
443	5808	5344	5813.2	9±0.05
551	5619	5078	5573	10±0.5
680	3790	3433	3773	10±0.3
688	1129	1010	1110	11±0.9
764	671.9	585.9	651.9	13±1.7
780	2794	2491	2799	12±0.1

325

Table 3B Global integral of reflected light ICs for the UTC of the Columbia, MO eclipse on 21 August and for the closest solar phase angle from 20 and 23 August. PD is the percent difference caused by the eclipse. Units are $ICs \times 10^{-7}$

λ_i (nm)	20 August 2017 18:03:359 GMT	21 August 2017 18:14:50	23 August 2017 17:54:36	Avg. PD
317.5	281.3	258.3	282.0	9±0.1
325	461.6	425.9	464.2	9±0.3
340	3193	2956	3213	8±0.3
388	2034	1884	2044	8±0.3
443	5813.7	5372.3	5813.2	8±0.01
551	5586	5091	5573	10±0.1
680	3790	3453	3773	10±0.2
688	1121	1011	1110	10±0.5
764	661.2	576.0	651.9	14±0.8
780	2794	2475	2799	13±0.1

326

327 Figure 9 shows a plot of the data contained in Table 3 based on Eqn. 1. The two non-eclipse days are
 328 nearly identical, while the eclipse day (21 Aug) is significantly lower at all wavelengths. The
 329 backscattered light (in C/s) peaks near 500 nm and then decreases toward longer wavelengths, since
 330 $C(\lambda)$ is proportional to the solar irradiance, which decreases with λ after approximately 550 nm.

$$ICs(\lambda) = \int_0^{2048} \int_0^{2048} C(\lambda, x, y) dx dy \tag{1}$$

over $N_p = 2.59 \times 10^6$ illuminated pixels on 20, 21, 23 August 2017

331

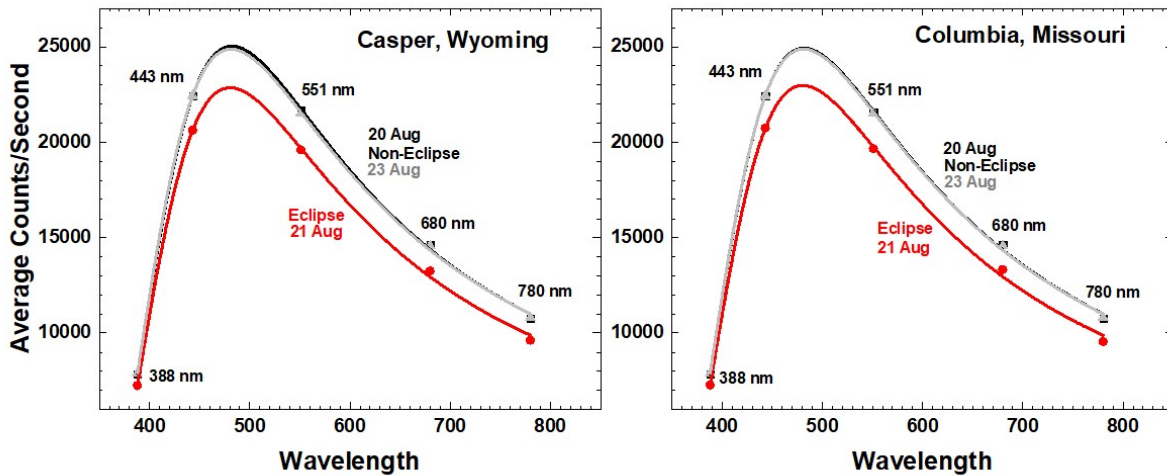


Fig. 9 Average $(ICs(\lambda)/N_p)$ reflected light in C/s for eclipse (21 Aug. red) and non-eclipse (20 Aug. and 23 Aug. (black and grey) days from Table 3 and Eqn. 1 for Casper and Columbia. The exact locations of the maxima are from curve fitting to the discrete wavelength measurements.

332

333 For the 443 nm channel, the result is an approximate decrease of 9 % on 21 August at 11:44:50
 334 for Casper and 8% at 12:14:50 for Columbia local time. As a reference, we compare two non-eclipse
 335 days (19 and 23 August). The relative difference is $(5808-5813)/5813$ 0.1 % for Casper and 0.01 % for
 336 Columbia, which is much smaller than the 9 % decrease produced by the eclipse on 21 August. The
 337 comparison of the 443 nm eclipse day with two non-eclipse days gives a measure of the uncertainty in
 338 the calculation (e.g., 9 ± 0.05 % for Casper and 8 ± 0.01 % for Columbia).

339

340 Percent difference $PD(\lambda_i)$ calculations for $\lambda_i = 317.5, 325, 340, 388, 443, 551, 680, 688, 764,$ and
 341 780 nm, based on Eqn. 1 are summarized in Table 3A, yielding $PD(\lambda_i) = 9, 9, 9, 9, 9, 9, 10, 10, 13,$ and 12
 342 % reductions in backscattered radiances in the direction of L_1 , respectively for Casper with similar values
 343 for Columbia. The $PD(764)$ within the strongly absorbing O_2 A-band is 13 % for Casper and 14% for
 344 Columbia, even though the reflected $ICs(764)$ is much lower than the surrounding non-absorbed bands.
 345 $PD(\lambda_i)$ is smaller at shorter wavelengths because of increased Rayleigh scattering that reduces the
 346 contrast of the Moon's shadow by scattering light into the umbra and penumbra regions from the areas
 347 adjacent to the total and partial eclipse. The fact that adjacent absorbed and non-absorbed wavelengths

348 give consistent $PD(\lambda_i)$ suggests that most of the effect comes from clouds and Rayleigh scattering and
 349 not from the relatively low reflectivity surface where the amount of clear-sky penetrating radiances are
 350 small for 688 and 764 nm channels.

351
 352 The TOA eclipse measurements made by EPIC are near the backscatter direction (172°) for the
 353 incident solar irradiance over nearly cloud-free scenes. For land surfaces, such as the observations made
 354 at Casper and Columbia, measurements from the POLDER satellite over China show that the backscatter
 355 amount from the land surface increases with increasing wavelength (Maignan et al., 2004). For EPIC data
 356 over land that are comparable to the POLDER measurements, the C/s data should be converted to
 357 reflectance. When this is done, the wavelength dependence of the EPIC albedo (551, 680, and 780 nm)
 358 is similar to POLDER surface reflectance even though there is no EPIC atmospheric correction and there
 359 is some cloud cover.

360

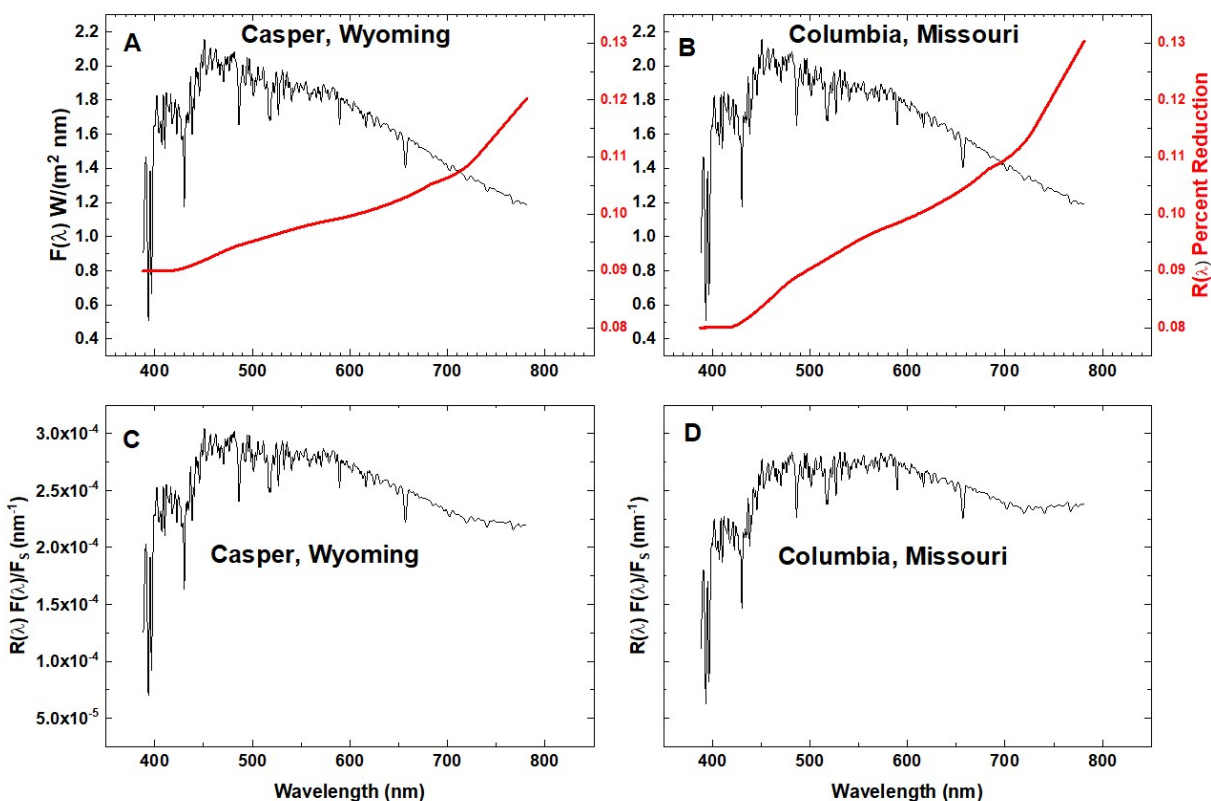


Fig. 10 Solar Irradiance at 1 AU $F(\lambda)$ Watts/($m^2 \text{ nm}$) (Mayer and Kylling, 2005) and the eclipse reduction function $R(\lambda)$ in percent for Casper, Wyoming (red curve in panel A) and Columbia, Missouri (red curve in panel B). Fractional reduction (nm^{-1}) in reflected solar irradiance in the direction of L-1 for Casper, Wyoming (panel C) and Columbia, Missouri (panel D)

361
 362 To estimate the fractional reflected radiance reduction for the wavelength range from 388 to
 363 780 nm, a polynomial interpolation $R(\lambda)$ of the Avg. PD in Table 3 for the 5 weakly absorbed channels is
 364 formed (Fig. 10 panels A and B red curves). $R(\lambda)$ must be weighted by the solar irradiance spectrum
 365 $F(\lambda)$. The solar spectrum used is a combination of measured solar flux data named "atlas_plus_modtran"

366 in the libRadtran software package (Mayer and Kylling, 2005). The components, F_R and F_S , of the
 367 weighted average R are defined in Eqns. 1 and 2. On 21 August 2017 the distance of the Earth from the
 368 Sun was 1.011 AU, or $F_S(21 \text{ Aug at } 1 \text{ AU}) = 664.94 \text{ W/m}^2$ and at 1 AU, $F_{R\text{-Casper}} = 66.11 \text{ W/m}^2$ and $F_{R\text{-Columbia}}$
 369 $= 64.86 \text{ W/m}^2$. For the wavelength range of interest (387.9 to 781.25 nm), F_S is about half of the total
 370 solar irradiance of 1361 W/m^2 at the top of the atmosphere at 1 AU (Kopp and Lean, 2011), where
 371
 372

$$F_S = \int_{387}^{781} F(\lambda) d\lambda \qquad F_R = \int_{387}^{781} R(\lambda) F(\lambda) d\lambda \qquad (2)$$

$$\langle R \rangle = \frac{\int_{387}^{781} R(\lambda) F(\lambda) d\lambda}{\int_{387}^{781} F(\lambda) d\lambda} \qquad R_{\text{Casper}} = 0.101 \qquad (3)$$

$$R_{\text{Columbia}} = 0.098$$

373 Figure 10b shows the product $R(\lambda)F(\lambda) / F_S$ (nm^{-1}). Forming R shows that during the eclipse the
 374 shadow of the Moon reduces the backscattered radiance (388 to 780 nm) from the sunlit Earth in the
 375 direction of L_1 by about 10 %. The combined uncertainty ± 0.3 % is caused by variations in the cloud
 376 cover of the reference days compared the eclipse day. The calculation of R is based on C/s
 377 measurements from DSCOVR/EPIC of the sunlit Earth and the interpolation function $R(\lambda)$. The result is
 378 independent of the absolute calibration of EPIC, since it is based on ratios of C/s over three days with
 379 approximately the same UTC (scattering phase angles). $R(\lambda)$ includes the near backscatter direction
 380 enhanced reflection function appropriate for the entire sunlit disk at a backscatter angle of about 172° .
 381 The three days at nearly the same UTC can be compared directly, since EPIC has proven to be very stable
 382 based on repeated in-flight calibrations over a 2-year period using OMPS and MODIS (Herman et al.,
 383 2018 and Geogdzhayev and Marshak, 2018). The smooth function $R(\lambda)$ does not include absorption
 384 features from water and the O_2 A- and B-bands.

385 3.0 Summary

386 The EPIC instrument onboard the DSCOVR spacecraft synoptically observes the entire sunlit
 387 portion of the Earth from an orbit near the Earth-Sun Lagrange-1 point. On 21 August 2017, EPIC was
 388 able to observe the totality shadow from the lunar eclipse of the Sun with the Earth's surface for about 3
 389 hours (seven 10-channel measurements) as it crossed the United States from west to east (about 1.5
 390 hours). When the region of totality was over Casper, Wyoming at 17:44:50 UTC, the reflected 443 nm
 391 TOA radiance was reduced to 16 C/s ($8 \times 10^{-5} \text{ W/m}^2 \text{sr}$) in the narrow region of totality compared to a non-
 392 eclipse day ($1.52 \times 10^4 \text{ C/s}$ or $0.076 \text{ W/m}^2 \text{sr}$). About 30 minutes later the shadow passed over Columbia,
 393 Missouri, but the presence of thin clouds in the vicinity of Columbia caused increased reflected radiance

394 of 312 C/s ($1.6 \times 10^{-3} \text{ W/m}^2 \text{sr}$) during totality compared to Casper. The ratio $R_{\text{EN}}(\lambda_i)$ of reflected radiances
395 within the eclipse totality to radiances for the same geometry on adjacent non-eclipse days was
396 measured for all 10 wavelength channels. The measured $R_{\text{EN}}(443 \text{ nm})$ was smaller for Columbia (71) than
397 for Casper (936), showing the sensitivity of increased cloud cover over Columbia. Similarly $R_{\text{EN}}(388 \text{ nm},$
398 $\text{Casper}) = 3500$ and $R_{\text{EN}}(388 \text{ nm}, \text{Columbia}) = 81$. While the results cannot be directly compared with
399 R_{EN} , good agreement was obtained (Kazantzidis et al., 2007) between a model study based on a 3D
400 Monte Carlo radiative transfer model (Emde and Mayer, 2007) and measured ratio at 380 nm (ratio =
401 217) of downward global surface radiation before and during totality. The measured radiance ratios
402 $R_{\text{EN}}(\lambda_i)$ can serve as a validation data set for 3D radiative transfer models of the atmosphere that include
403 cloud effects, since EPIC also measures the surrounding amount of cloud cover for the entire sunlit
404 Earth. Comparing $R_{\text{EN}}(\lambda, \text{Casper})$ with $R_{\text{EN}}(\lambda, \text{Columbia})$ shows that Rayleigh scattering combined with
405 low optical depth clouds can scatter light into the umbra region and reduce $R_{\text{EN}}(\lambda)$. Outside of the region
406 of totality, EPIC observed the partial eclipse shadow and the fully illuminated regions of the Earth's disk.
407 Interpolating between the percent reductions in integrated radiances (in C/s) over the sunlit globe,
408 $\text{ICs}(\lambda_i)$ for the 5 measured non-absorbed wavelength channels at both locations showed that the
409 integrated reflected radiance from the Earth's sunlit disk towards L_1 decreased by about 10 % compared
410 to the integrated radiances measured on the days before and after the eclipse for approximately the
411 same observing geometry as occurred during the eclipse. Similar calculations comparing two non-eclipse
412 days show smaller changes in ICs (less than 0.1 %) than the eclipse-day change. The five channels that
413 are partially absorbed in the atmosphere give consistent results compared to the non-absorbed
414 channels suggesting that cloud reflectivities dominate the 317.5 to 780 nm radiances reflected back to
415 space from the sunlit Earth's disk with a contribution from Rayleigh scattering for the shorter
416 wavelengths.

417

418 **Appendix**

419 The course of the eclipse in the vicinity of Casper, Wyoming and Columbia, Missouri is shown in Fig. A1

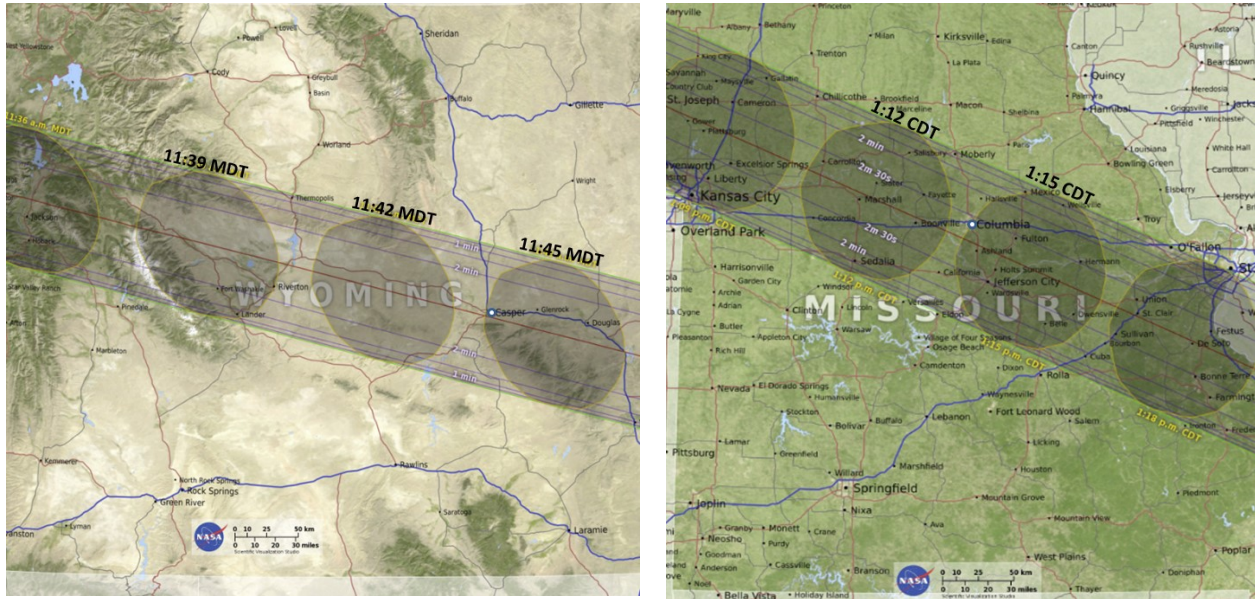


Fig. A1 The timing and shape of the Moon’s shadow over Casper, Wyoming showing the relative location of Casper and Columbia (white circles) at 11:45 MDT (Mountain Daylight Time) and 1:15 CDT (Central Daylight Time). The shadow is moving at about 46 km/minute. (<https://eclipse2017.nasa.gov/eclipse-maps>). The NASA scale size is 50 km.

420

421

422

423 Greyscale images for the short UV wavelength channels (317.5, 325) with strong ozone absorption and
424 Rayleigh scattering, the longer wavelength UV channels (340, 388), and the strongly absorbed O₂ B- and
425 A-band channels (688, 764 nm) are shown in Figs. A2a, A2b, A2c

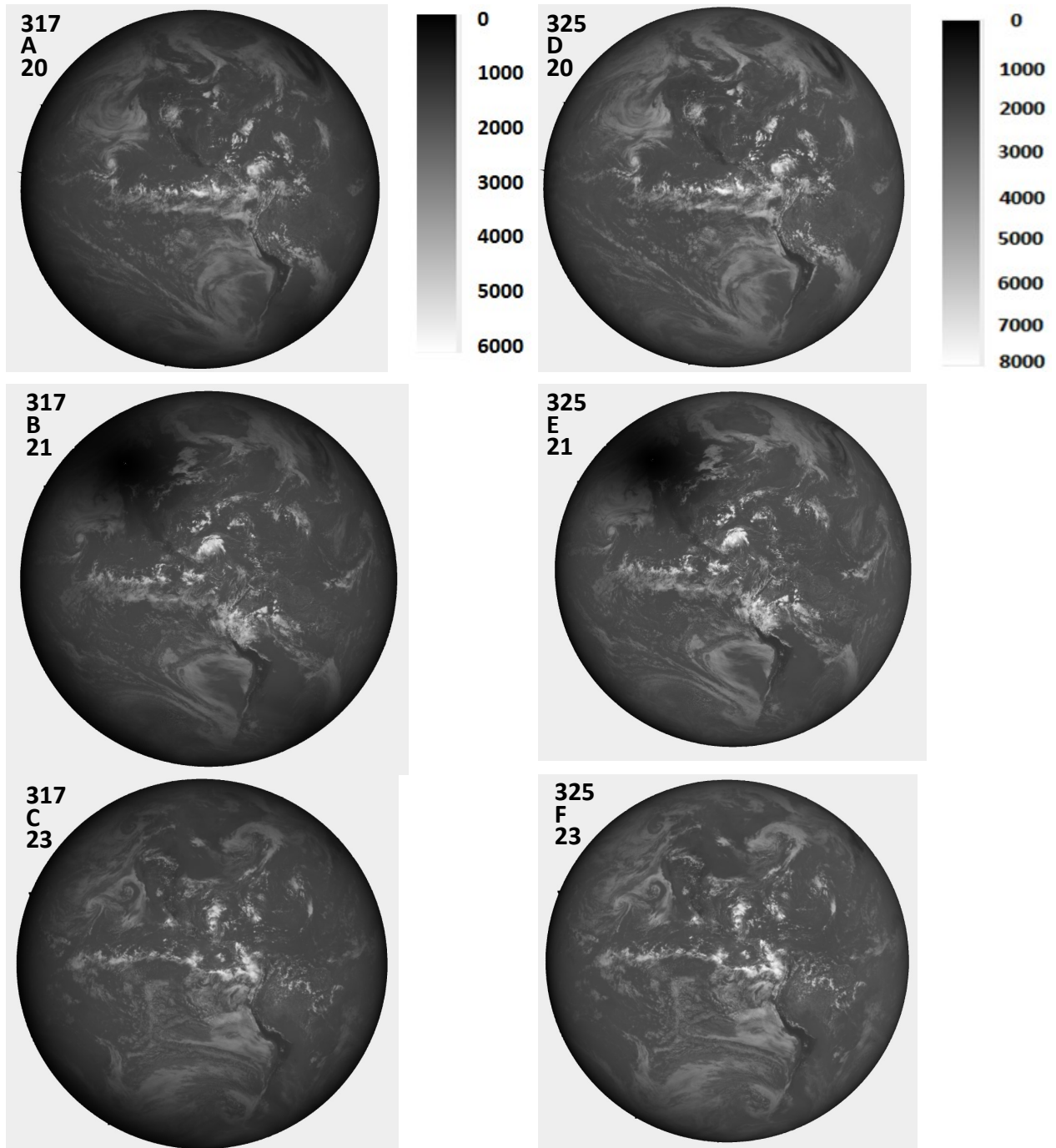


Fig. A2a Image in C/s for 317 and 340 nm for 20 Aug., 21 Aug. and 23 Aug. The scale applies to the specific wavelength. North is up.

426

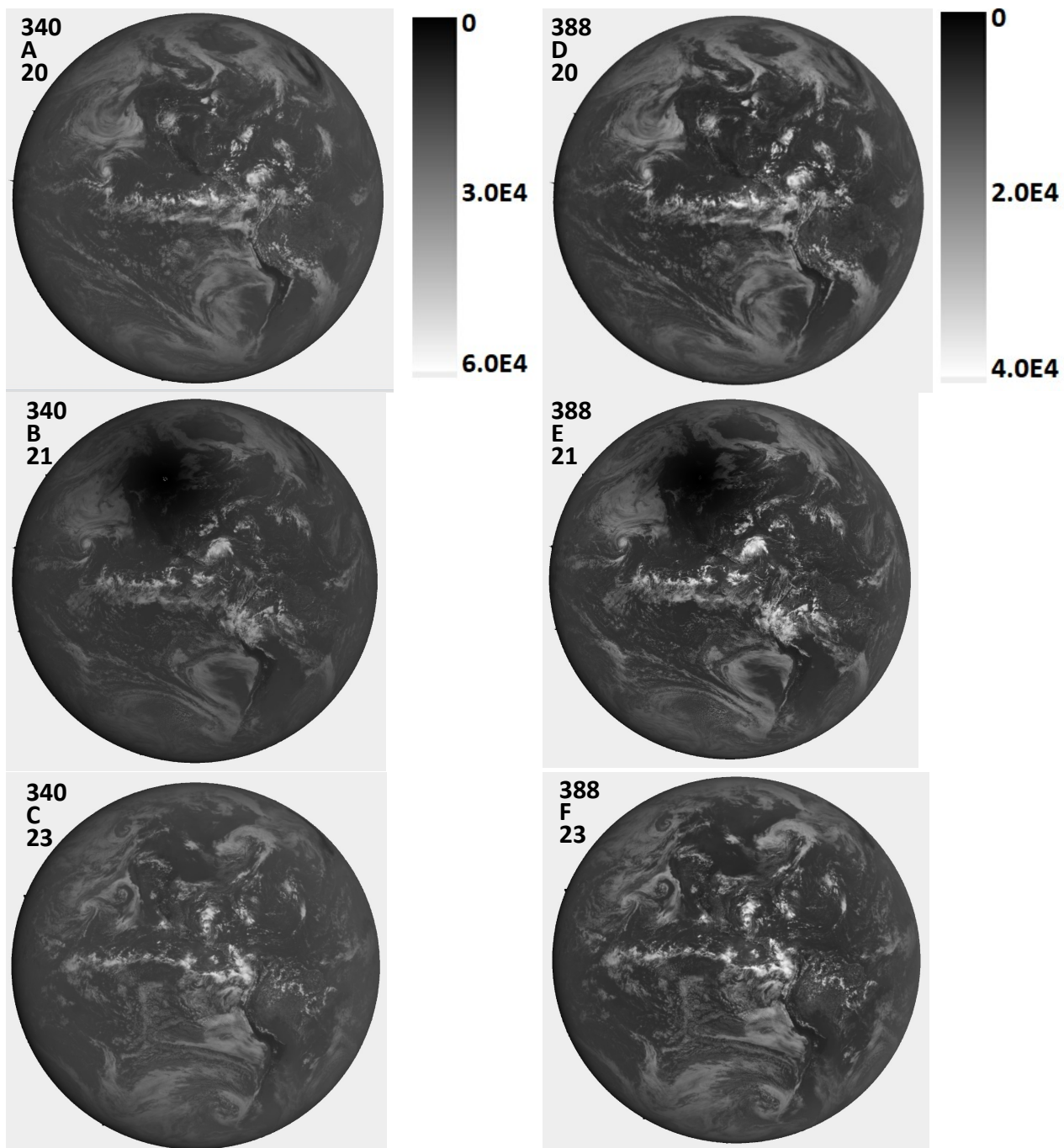


Figure A2b Image in C/s for 340 and 388 nm for 20 Aug.(A+C), 21 Aug. (B+E), and 23 Aug. (C+F). The scale applies to the specific wavelength. North is up.

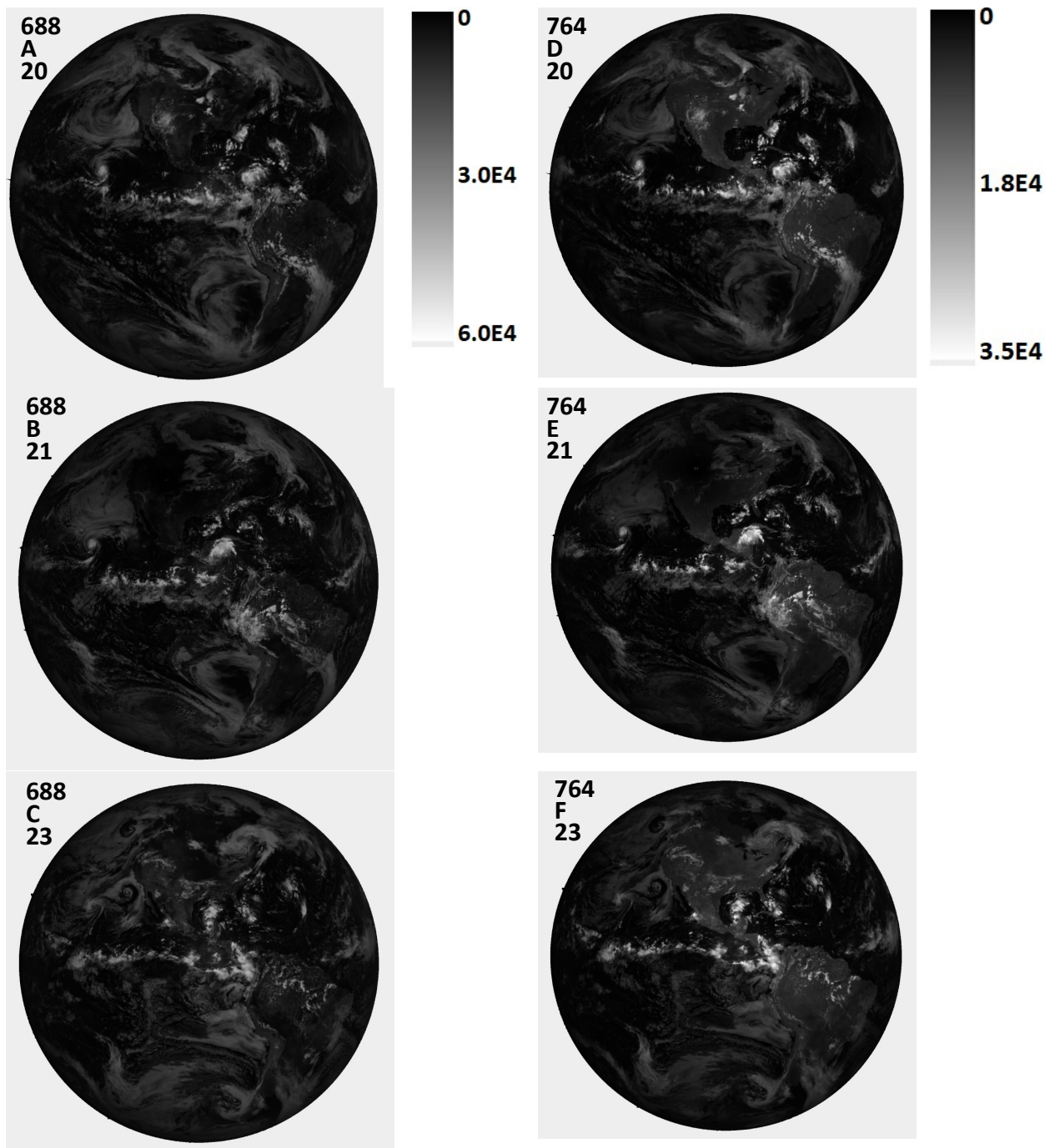


Fig. A2c Image in C/s for 688 and 764 nm for 20 Aug., 21 Aug. and 23 Aug. The scale applies to the specific wavelength. North is up.

429

430 The amount of ozone over the eclipse sites can be derived (Herman et al., 2018) to produce
 431 ozone data that is stored in the NASA-Langley archive. During the eclipse, it is not possible to derive the
 432 amount of ozone from either ground-based or satellite data. Ozone amounts do not change rapidly from
 433 day to day except when major weather systems pass through a region, which was not the case during

434 the eclipse period, 20 August to 23 August. This is confirmed from OMI satellite data (Ozone Monitoring
435 Instrument onboard the AURA satellite). Figure A3 shows the amount of ozone over the eclipse
436 trajectory obtained on 20 August. The values obtained 316 DU near Casper, WY and 306 DU near
437 Columbia compare well with ozone amounts derived from OMI of 314 DU and 301 DU. The O₃ variability
438 during the 2.7 minutes (approximately 124 km or about 1° of longitude) is about ±5 DU.

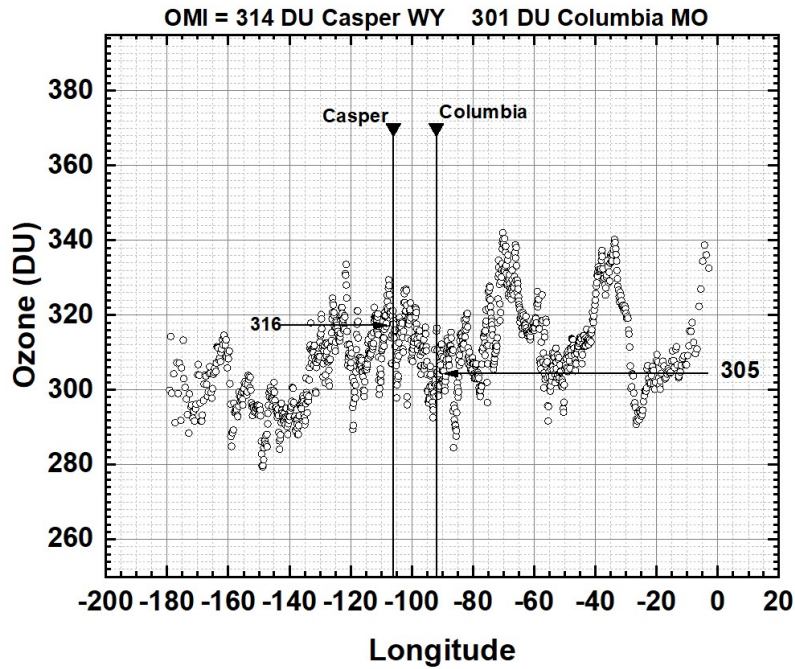


Fig. A3 EPIC measured ozone amounts from 20 August in the vicinity of Casper, WY and Columbia, MO.

439

440

441

442 **4.0 Author Contributions**

443 Jay Herman wrote most of the paper and performed most of the calculations

444 Guoyong Wen is the funded principal investigator of the project.

445 Alexander Marshak provided the calibration coefficients for the visible and near-IR channels

446 Karin Blank provided the color images in Figs. 1 to 3. She was responsible for the geolocation of the 10
447 filter images on a common grid.

448 Liang Huang provided the calibration coefficients for the UV channels

449 Alexander Cede provided the flatfielding, stray light correction, and dark current analysis

450 Nader Abuhassan helped with flatfielding and stray light correction and was responsible for the ground-
451 based portion of this research.

452 Matthew Kowalewski provided the flatfielding, stray light correction, and dark current analysis

453

454

455 The authors declare that they have no conflict of interest.

456 **5.0 References**

457 Cleveland, William S., LOWESS: A program for smoothing scatterplots by robust locally weighted
458 regression. *The American Statistician*. **35** (1): 54. [JSTOR 2683591](https://doi.org/10.2307/2683591). doi:10.2307/2683591, 1981.

459
460 Emde, C. and B. Mayer, Simulation of solar radiation during a total eclipse: a challenge for radiative
461 transfer,(2007) *Atmos. Chem. Phys.*, **7**, 2259–2270, 2007.

462 Geogdzhayev, I. V. and Marshak, A.: Calibration of the DSCOVR EPIC visible and NIR channels using
463 MODIS Terra and Aqua data and EPIC lunar observations, *Atmos. Meas. Tech.*, **11**, 359-368,
464 <https://doi.org/10.5194/amt-11-359-2018>, 2018.

465 Gerasopoulos, E., Zerefos, C. S., Tsagouri, I., Founda, D., Amiridis, V., Bais, A. F., Belehaki, A., Christou, N.,
466 Economou, G., Kanakidou, M., Karamanos, A., Petrakis, M., and Zanis, P.: The total solar eclipse of March
467 2006: overview, *Atmos. Chem. Phys.*, **8**, 5205-5220, <https://doi.org/10.5194/acp-8-5205-2008>, 2008.

468 Herman, J.R., Alexander Cede, Elena Spinei, George Mount, Maria Tzortziou, Nader Abuhassan, (2009)
469 NO₂ Column Amounts from Ground-based Pandora and MFDOAS Spectrometers using the Direct-Sun
470 DOAS Technique: Intercomparisons and Application to OMI Validation, *J. Geophys. Res.*, **114**, D13307,
471 doi:10.1029/2009JD011848, 2009.

472
473 Herman, J.R., R.D. Evans, A. Cede, N.K. Abuhassan, I. Petropavlovskikh, and G. McConville, (2015)
474 Comparison of Ozone Retrievals from the Pandora Spectrometer System and Dobson
475 Spectrophotometer in Boulder Colorado, *Atmos. Meas. Tech.*, **8**, 3407–3418, 2015 doi:10.5194/amt-8-
476 3407-2015

477
478 Herman, Jay, Liang Huang, Richard McPeters, Jerry Ziemke, Alexander Cede, and Karin Blank, Synoptic
479 ozone, cloud reflectivity, and erythemal irradiance from sunrise to sunset for the whole earth as viewed
480 by the DSCOVR spacecraft from the earth–sun Lagrange 1 orbit, 2017, *Atmos. Meas. Tech.*, **10**, 1–18,
481 <https://doi.org/10.5194/amt-10-1-2017>.

482 Ji, Q. and S.-C. Tsay (2000) On the dome effect of Eppley pyrgeometers and pyranometers, *Geophys.*
483 *Res. Lett.* **27**:971-974.

484 Kazantzidis, A., Bais, A. F., Emde, C., Kazadzis, S., and Zerefos, C. S.: Attenuation of global ultraviolet and
485 visible irradiance over Greece during the total solar eclipse of 29 March 2006, *Atmos. Chem. Phys.*, **7**,
486 5959-5969, <https://doi.org/10.5194/acp-7-5959-2007>, 2007.

487 Kopp, G.; Lean, J. L., (2011), A new, lower value of total solar irradiance: Evidence and climate
488 significance, *Geophysical Research Letters*. **38**.

489 Littmann, Mark; Espenak, Fred; *Wilcox*, Ken (2008). *Totality: Eclipses of the Sun*. Oxford University
490 Press. pp. 18–19. ISBN 0-19-953209-5.

491 Liendo, J.A. and G.H. Chacin, (2004), A study of a solar eclipse using a photocell, *Revista Brasileira de*
492 *Ensino de Fisica*, v. 26, 395 – 399.

493 Maignan, F., Breon, F. M., and Lacaze, R., (2004), Bidirectional reflectance of Earth targets: Evaluation of
494 analytical models using a large set of spaceborne measurements with emphasis on the Hot Spot,
495 Remote Sens. Environ., 90, 210–220, doi:10.1016/j.rse.2003.12.006.

496 Marshak, Alexander, Jay R. Herman, Adam Szabo, Karin B. Blank, Alexander Cede, Simon A. Carn, Igor V.
497 Geogdzhayev, Dong Huang, Liang-Kang Huang, Yuri Knyazikhin, Matthew G. Kowalewski, Nickolay A.
498 Krotkov, Alexei I. Lyapustin, Richard D. McPeters, Omar O. Torres and Yuekui Yang, Earth Observations
499 from DSCOVR/EPIC Instrument, BAMS, accepted, 2018

500

501 Mayer, B. and Kylling, (2005) A.: Technical Note: The libRadtran software package for radiative transfer
502 calculations: Description and examples of use, Atmos. Chem. Phys., 5, 1855–1877, [http://www.atmos-](http://www.atmos-chem-phys.net/5/1855/2005/)
503 [chem-phys.net/5/1855/2005/](http://www.atmos-chem-phys.net/5/1855/2005/).

504

505 Meeus, J. (2003). "The maximum possible duration of a total solar eclipse". *Journal of the British*
506 *Astronomical Association*. **113** (6): 343–48.

507 Psiloglou, B.E. and H. D. Kambezidis, Performance of the meteorological radiation model during the solar
508 eclipse of 29 March 2006, Atmos. Chem. Phys., 7, 6047–6059, 2007.

509 Wen, G., A. Marshak, and R.F. Cahalan, (2008) Importance of molecular Rayleigh scattering in the
510 enhancement of clear sky radiance in the vicinity of boundary layer cumulus clouds. *J. Geophys. Res.*,
511 113: [10.1029/2008JD010592].

512

513

514 Acknowledgement

515 The author would like to thank the DSCOVR project for support in completing this study as well as
516 financial support from an accepted NASA-ROSES proposal in response to NNH16ZDA001N-ISE. All data is
517 from the permanent NASA data repository:

518 https://eosweb.larc.nasa.gov/project/dscovr/dscovr_epic_l1b.

519

520 **Tables**

521

Table 1 *Eclipse Measurement Timing and Location Details for 5 Wavelengths*

Eclipse Maximum and EPIC Image Times. Total Measurement Duration 2.7 minutes

Wavelength (nm)	Date and Time	Location Name	Longitude
	2017-08-21 17:35:40	Eclipse West Edge of WY state	-111 ⁰ 02'
551	2017-08-21 17:42:36	West of Casper	-106 ⁰ 22'
680	2017-08-21 17:43:30	West of Casper	-106 ⁰ 21'
Casper Wyoming	2017-08-21 17:43:51	Casper WY	-106 ⁰ 19'
780	2017-08-21 17:44:24	Near Glenrock WY	-105 ⁰ 52'
443	2017-08-21 17:44:50	West of Douglas WY	-105 ⁰ 14'
388	2017-08-21 17:45:18	West of Douglas WY	-105 ⁰ 17'
	2017-08-21 17:48:04	Eclipse East Edge of WY state	-104 ⁰ 03'

522

523

524

Table 2 *Radiance Ratio $R_{EN}(\lambda_i)$ during eclipse totality 17:45 UTC compared to 20 Aug*

Wavelength λ_i (nm)	Max. $R_{EN}(\lambda_i)$ C/s
317.5	118
325	68.2
340	144
388	86
443	122
551	119.5
680	80
688	38
764	108
780	112.5

525

526

527

528

529

530

531

532

Table 3A Eclipse change in reflected light at Casper, WY from 20, 21, 23 August 2017 Units are ICs x 10⁻⁷

λ_i (nm)	20 August 2017 16:58:31 GMT	21 August 2017 17:44:50	23 August 2017 17:54:36	Avg. PD
317.5	280.5	258.8	282.0	9±0.3
325	460.6	425.5	464.2	9±0.4
340	3183	2946	3213	9±0.5
388	2034	1878	2044	9±0.3
443	5808	5344	5813.2	9±0.05
551	5619	5078	5573	10±0.5
680	3790	3433	3773	10±0.3
688	1129	1010	1110	11±0.9
764	671.9	585.9	651.9	13±1.7
780	2794	2491	2799	12±0.1

533

Table 3B Eclipse change in reflected light at Columbia, MO from 20, 21, 23 August 2017 Units are ICs x 10⁻⁷

λ_i (nm)	20 August 2017 18:03:359 GMT	21 August 2017 18:14:50	23 August 2017 17:54:36	Avg. PD
317.5	281.3	258.3	282.0	9±0.1
325	461.6	425.9	464.2	9±0.3
340	3193	2956	3213	8±0.3
388	2034	1884	2044	8±0.3
443	5813.7	5372.3	5813.2	8±0.01
551	5586	5091	5573	10±0.1
680	3790	3453	3773	10±0.2
688	1121	1011	1110	10±0.5
764	661.2	576.0	651.9	14±0.8
780	2794	2475	2799	13±0.1

534

535

536

537

538 **Figure Captions**

539 Fig. 1 Synoptic view of the sunlit Earth perturbed by the 21 August 2017 total eclipse centered over
540 Casper, Wyoming at 17:44:50 UTC. The black region is the eclipse umbra centered over Casper, WY. The
541 color image has been adjusted from the images on <https://epic.gsfc.nasa.gov/>
542 by increasing the gamma correction to bring out the region of totality and surrounding clouds.

543 Fig. 2 Synoptic view of the total eclipse centered over Columbia, Missouri at 18:14:50 UTC. The black
544 region is the eclipse umbra centered over Casper, WY. The color image has been adjusted from the
545 images on <https://epic.gsfc.nasa.gov/> by increasing the gamma correction to bring out the region of
546 totality and surrounding clouds.

547 Fig. 3 Greyscale images for 6 of the DSCOVR/EPIC channels for the eclipse over Casper Wyoming
548 showing the blurring caused by Rayleigh scattering and the dark land and ocean surfaces at 340 nm to
549 the almost clear atmosphere and bright continental surfaces at 780 nm. The images were obtained over
550 a period of 2.7 minutes. North is facing down.

551 Fig. 4 Panel A: Synoptic natural color images on 21 August at 16:14 and 19:44 before and after the
552 eclipse over the US, and Panel B: the days before and after the eclipse selected to be as close as possible
553 to the phase angle (UTC 17:44:50) as the time of totality over Casper, Wyoming. North is facing up.

554 Fig. 5 Top: The effect of an eclipse (21 Aug) on the measured C/s reflected back to space as a function of
555 longitude (degrees) for two locations, Casper Wyoming (left) and Columbia Missouri (right). Bottom:
556 Measured C/s reflected back to space on 20 Aug. A \log_{10} scale is used to show details of the spatial
557 variability mostly caused by clouds

558 Figure . The ratio $R_{EN}(\lambda_i) = I(\text{Aug20})/I(\text{Aug21})$ at the time of the Eclipse in Casper Wyoming for
559 wavelengths 317.5 to 780 nm. The channels 317.5 to 240 nm are affected by ozone absorption and the
560 channels 688 and 764 nm are within the O₂ B and A absorption bands.

561 Fig. 6b The ratio $R_{EN}(\lambda_i) = I(\text{Aug20})/I(\text{Aug21})$ at the time of the Eclipse in Columbia, Missouri for
562 wavelengths 317.5 to 780 nm. The channels 317.5 to 340 nm are affected by ozone absorption and the
563 channels 688 and 764 nm are within the O₂ B and A absorption bands.

564 Fig. 7 The C/s observed by EPIC for the 443 nm channel corresponding to the color image shown in Fig.
565 1. In the data file, the word infinity has been replaced by the number zero. In this image there are
566 approximately $N_p = 2.59 \times 10^6$ illuminated pixels out of $2048^2 = 4.194304 \times 10^6$ pixels (61.8 %).

567 Fig. 8a Figure 8b Image in C/s for 443 and 551 nm for 20 Aug.(A+C), 21 Aug. (B+E), and 23 Aug. (C+F). The
568 scale applies to the specific wavelength. North is up.

569 Fig. 8b Figure 8c Image in C/s for 680 and 780 nm for 20 Aug.(A+C), 21 Aug. (B+E), and 23 Aug. (C+F). The
570 scale applies to the specific wavelength. North is up

571 Fig. 9 Average reflected light in C/s for eclipse (21 Aug. red) and non-eclipse (20 Aug. and 23 Aug. (black
572 and grey) days from Table 3 and Eqn. 1 for Casper and Columbia. The locations of the maxima are from
573 curve fitting to the discrete wavelength measurements.

574 Fig. 10 Solar Irradiance at 1 AU $F(\lambda)$ Watts/(m² nm) (Mayer and Kylling, 2005) and the eclipse reduction
575 function $R(\lambda)$ in percent for Casper, Wyoming (red curve in panel A) and Columbia, Missouri (red curve
576 in panel B). Fractional reduction (nm⁻¹) in reflected solar irradiance in the direction of L-1 for Casper,
577 Wyoming (panel C) and Columbia, Missouri (panel D)

578 Fig. A1 The timing and shape of the Moon's shadow over Casper, Wyoming showing the relative location
579 of Casper and Columbia (white circles) at 11:45 MDT (Mountain Daylight Time) and 1:15 CDT (Central
580 Daylight Time). The shadow is moving at about 46 km/minute. ([https://eclipse2017.nasa.gov/eclipse-
581 maps](https://eclipse2017.nasa.gov/eclipse-
581 maps)). The NASA scale size is 50 km.

582 Fig. A2a Image in C/s for 317 and 340 nm for 20 Aug., 21 Aug. and 23 Aug. The scale applies to the
583 specific wavelength. North is up.

584 Fig. A2b Image in C/s for 340 and 388 nm for 20 Aug.(A+C), 21 Aug. (B+E), and 23 Aug. (C+F). The scale
585 applies to the specific wavelength. North is up.

586 Fig. A2c A2c Image in C/s for 688 and 764 nm for 20 Aug., 21 Aug. and 23 Aug. The scale applies to the
587 specific wavelength. North is up.

588 Fig. A3 EPIC measured ozone amounts from 20 August in the vicinity of Casper, WY and Columbia, MO.

589

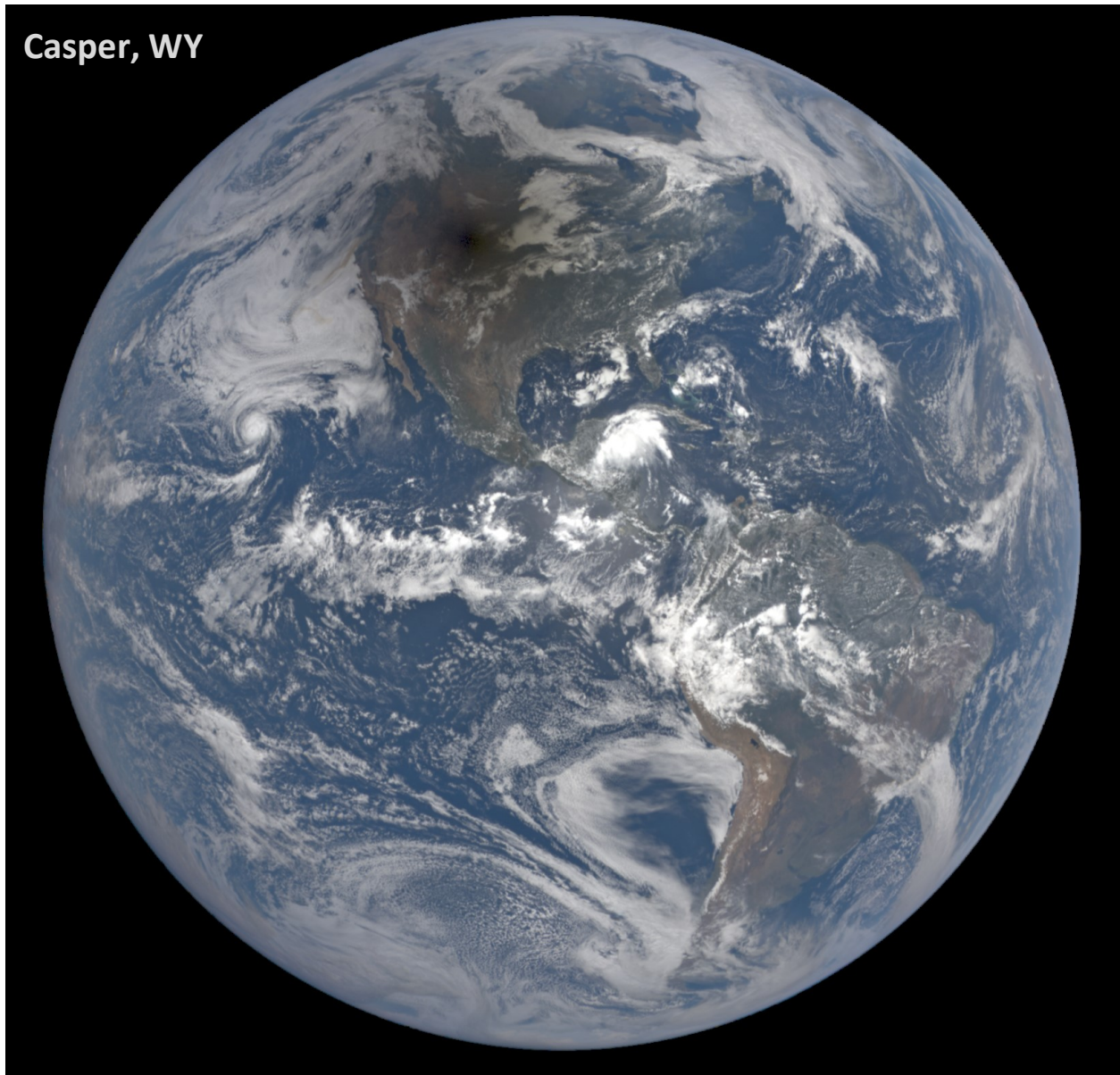


Fig. 1 Synoptic view of the sunlit Earth perturbed by the 21 August 2017 total eclipse centered over Casper, Wyoming at 17:44:50 UTC. The black region is the eclipse umbra centered over Casper, WY. The color image has been adjusted from the images on <https://epic.gsfc.nasa.gov/> by increasing the gamma correction to bring out the region of totality and surrounding clouds.

590

591

592 **F01**

593



Fig. 2 Synoptic view of the total eclipse centered over Columbia, Missouri at 18:14:50 UTC. The black region is the eclipse umbra centered over Casper, WY. The color image has been adjusted from the images on <https://epic.gsfc.nasa.gov/> by increasing the gamma correction to bring out the region of totality and surrounding clouds.

594

595

596 **F02**

597

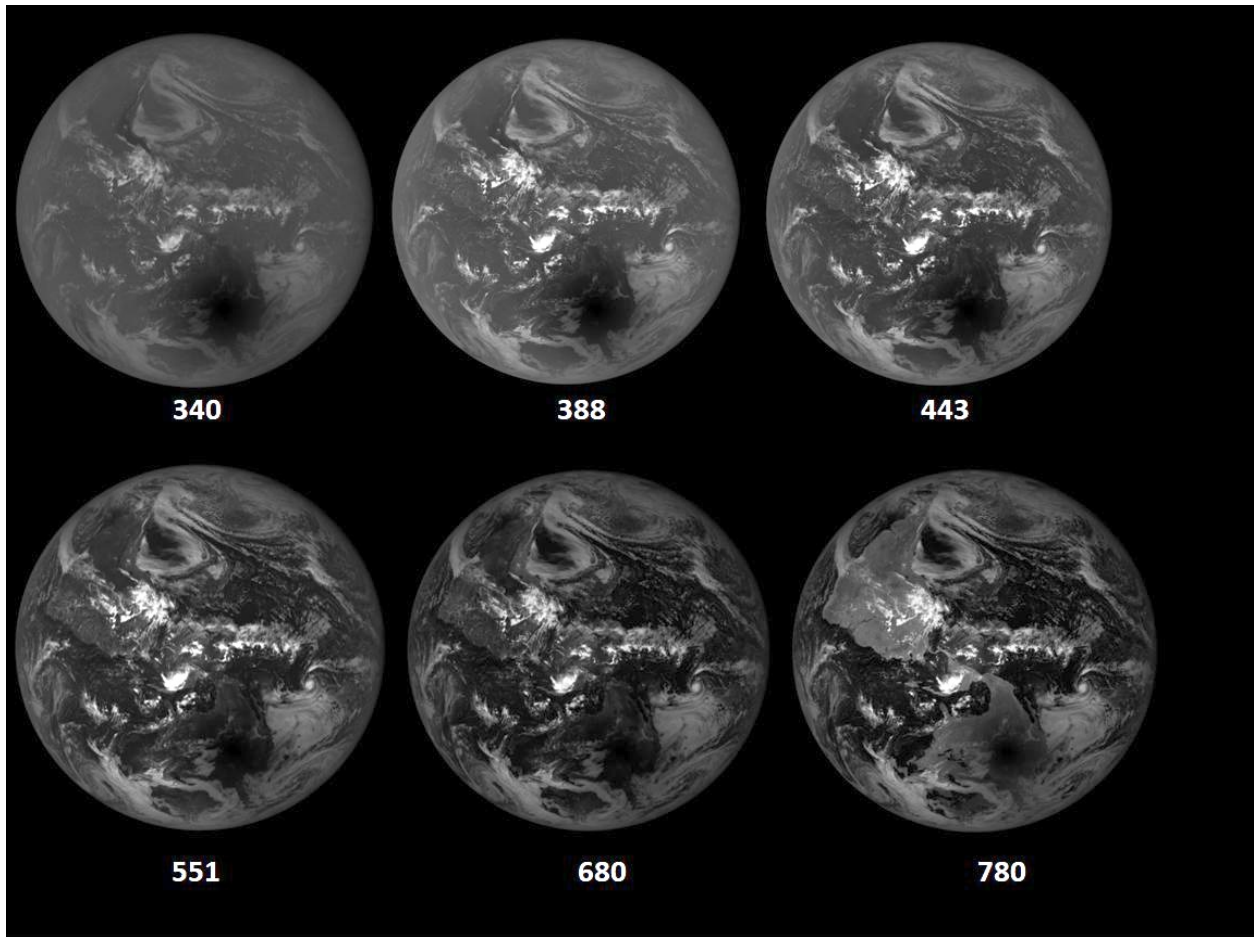


Fig. 3 Greyscale images for 6 of the DSCOVR/EPIC channels for the eclipse over Casper Wyoming showing the blurring caused by Rayleigh scattering and the dark land and ocean surfaces at 340 nm to the almost clear atmosphere and bright continental surfaces at 780 nm. The images were obtained over a period of 2.7 minutes. North is facing down.

598

599

600 **F03**

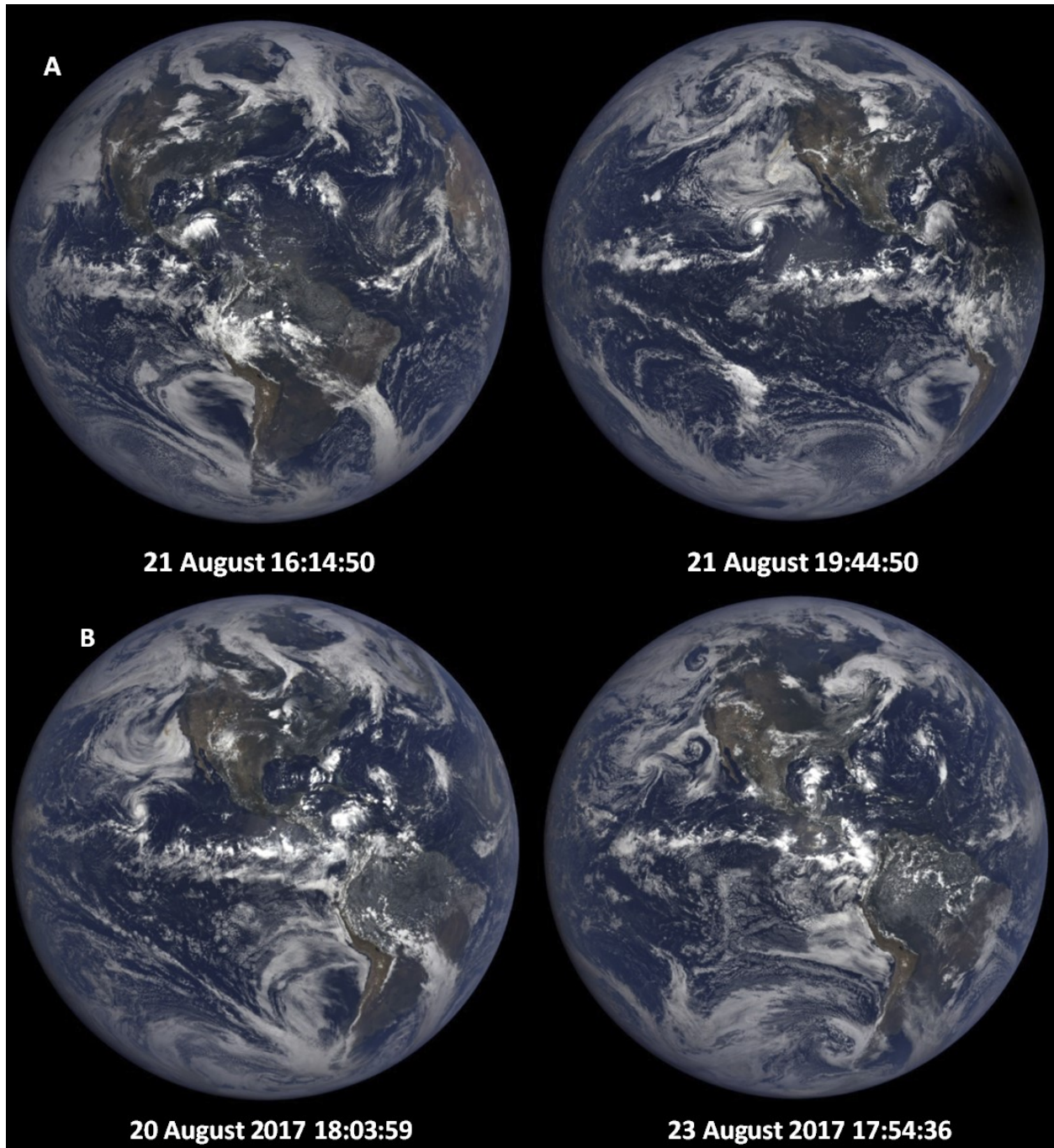


Fig. 4 Panel A: Synoptic natural color images on 21 August at 16:14 and 19:44 before and after the eclipse over the US, and Panel B: the days before and after the eclipse selected to be as close as possible to the phase angle (UTC 17:44:50) as the time of totality over Casper, Wyoming. North is facing up.

601

602 **F04**

603

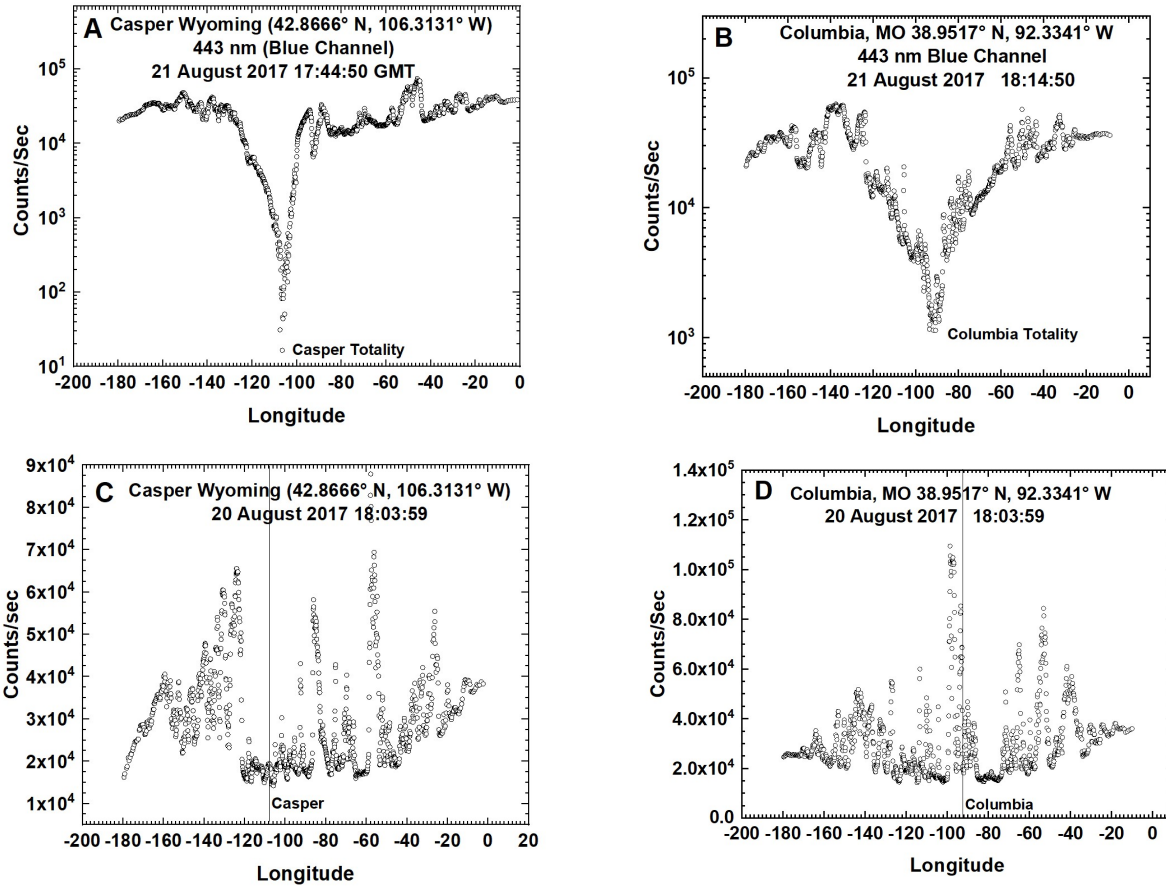


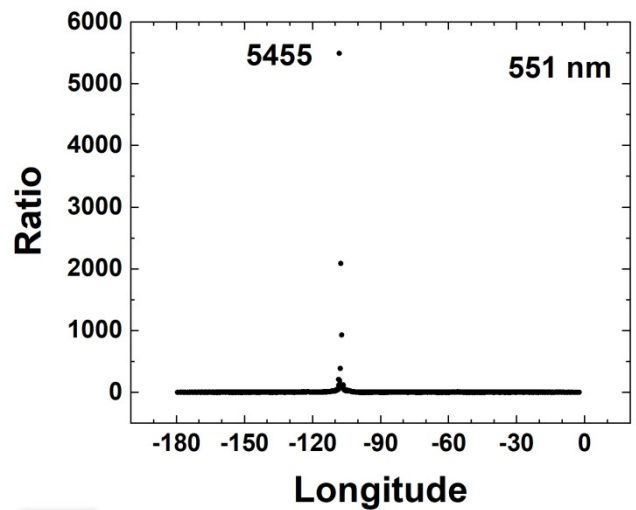
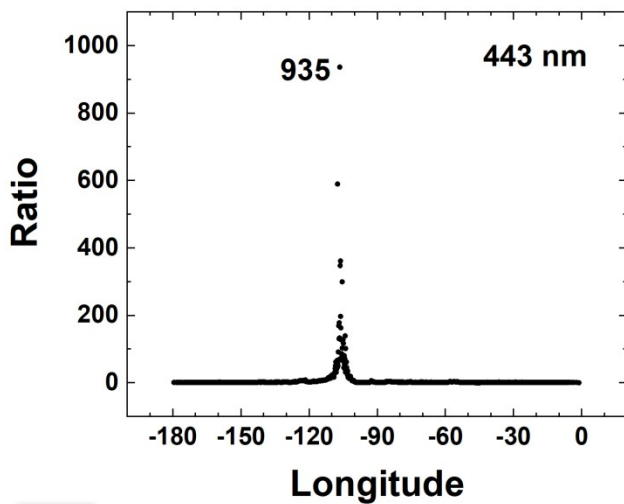
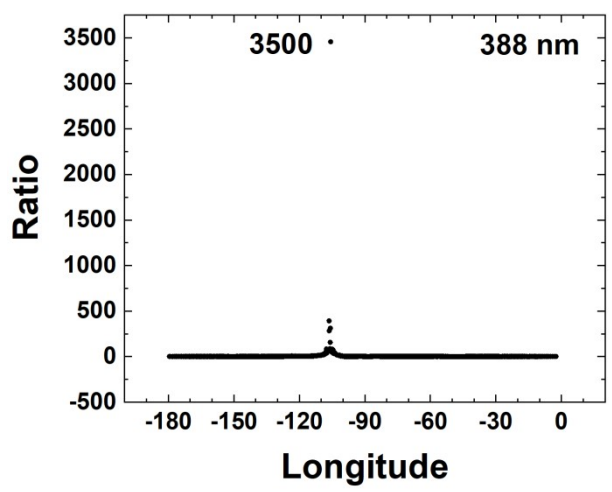
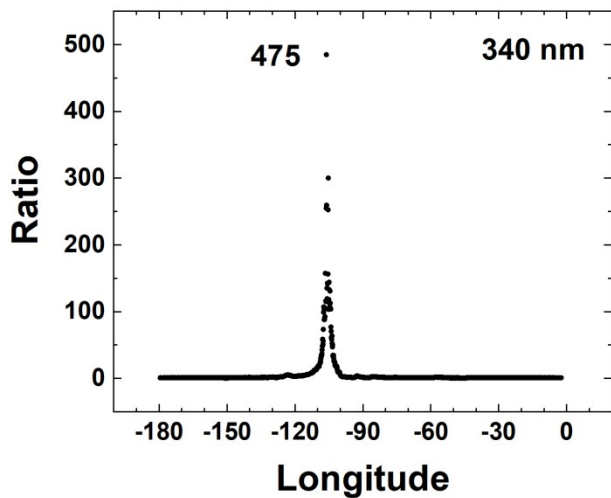
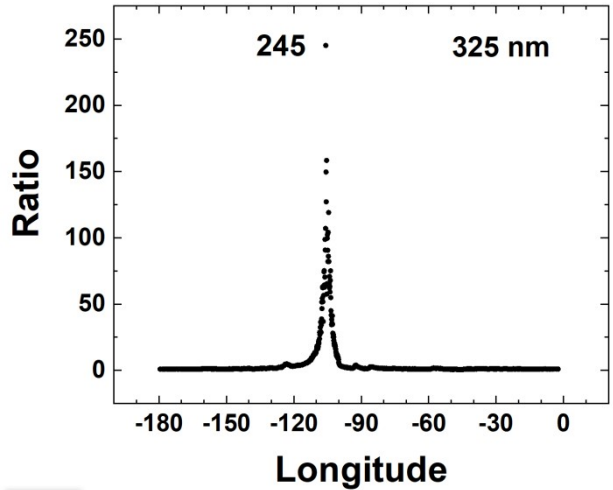
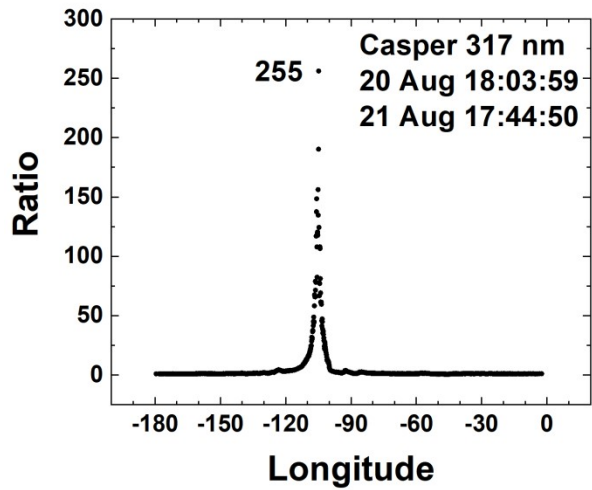
Fig. 5 Top: The effect of an eclipse (21 Aug) on the measured C/s reflected back to space as a function of longitude (degrees) for two locations, Casper Wyoming (left) and Columbia Missouri (right). Middle: Measured C/s reflected back to space on 20 Aug.

604

605

606 **F05**

607



608

609 F06a

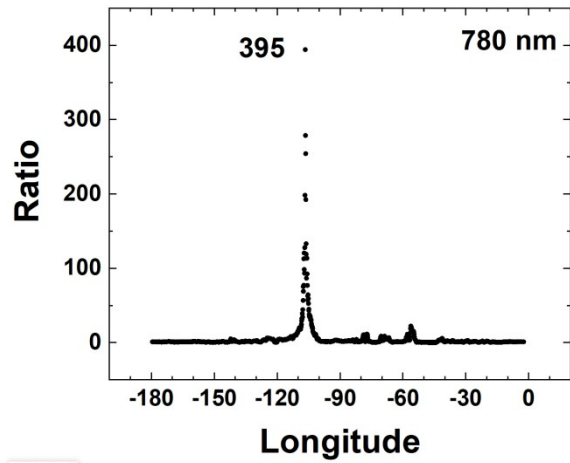
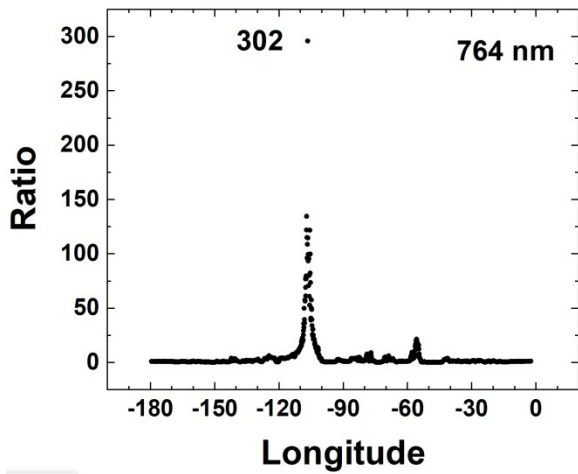
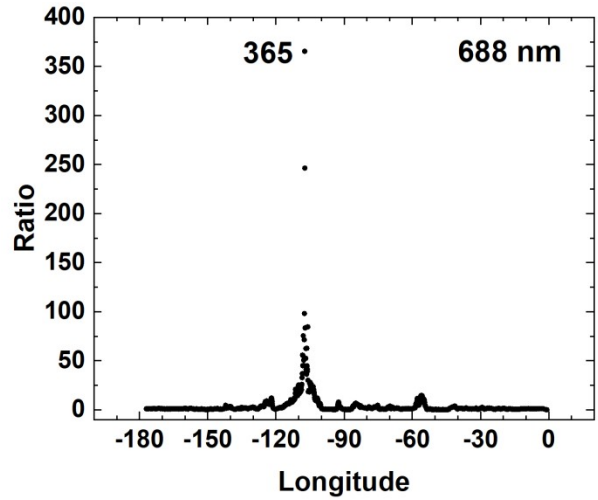
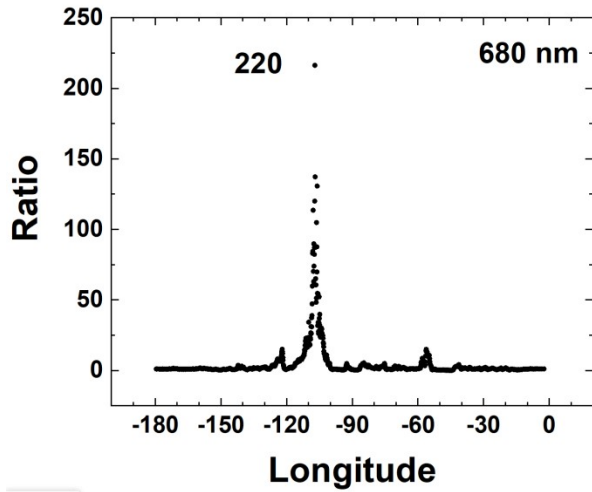
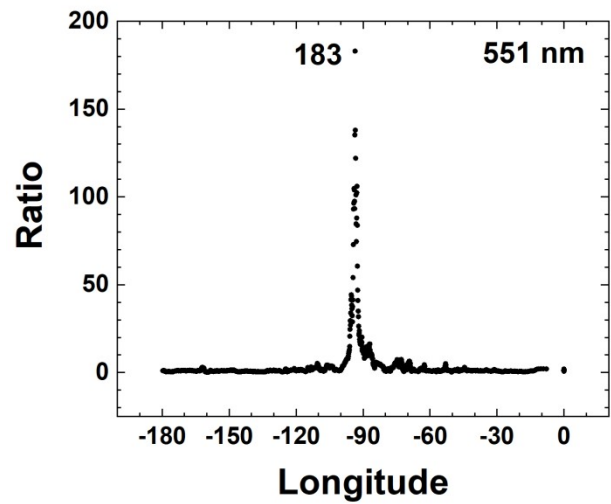
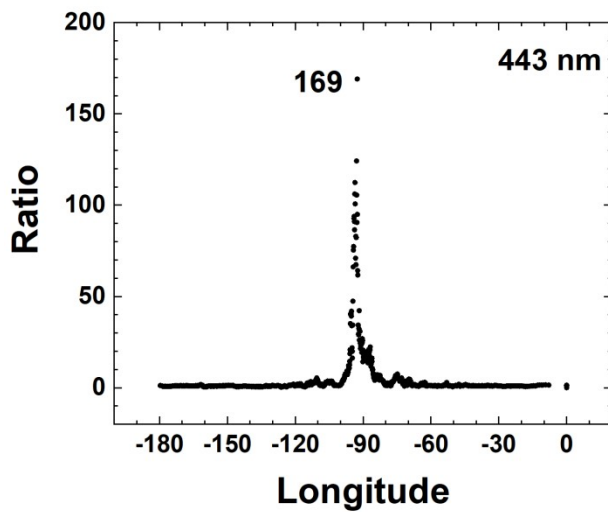
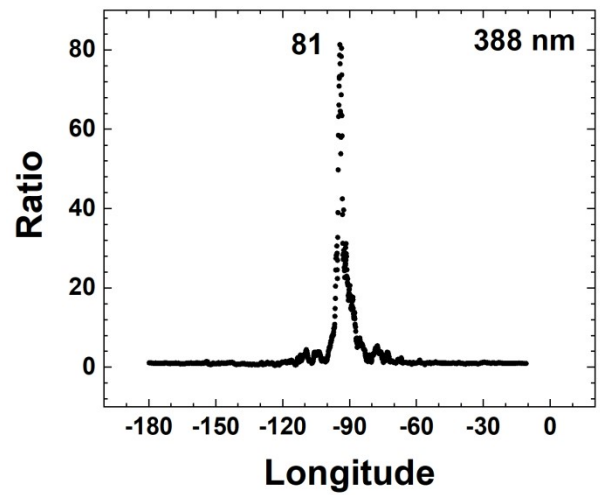
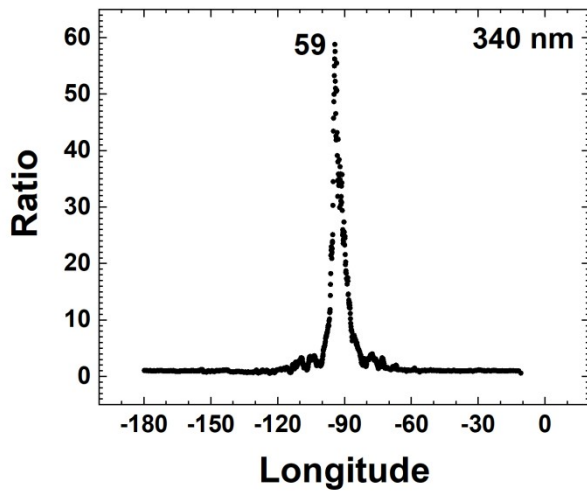
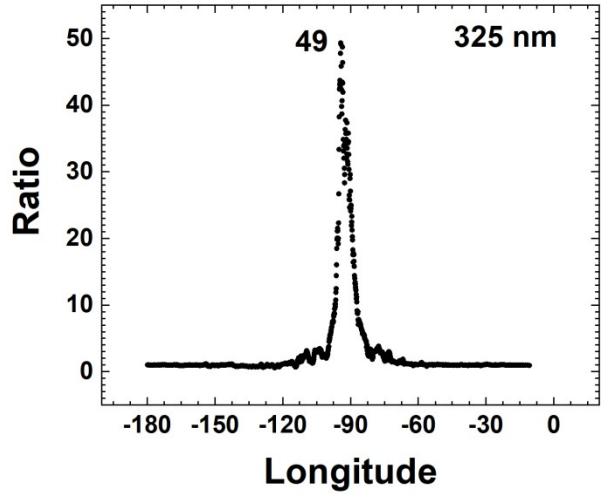
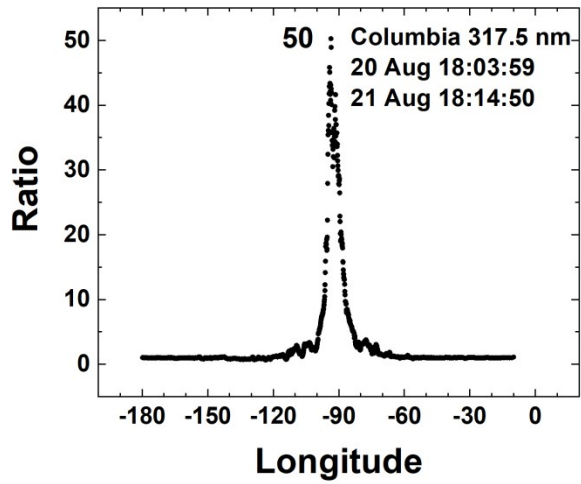


Fig. 6a. The ratio $R_{EN}(\lambda_i) = I(\text{Aug20})/I(\text{Aug21})$ at the time of the Eclipse in Casper Wyoming for wavelengths 317.5 to 780 nm. The channels 317.5 to 240 nm are affected by ozone absorption and the channels 688 and 764 nm are within the O_2 B and A absorption bands.

610

611

612 **F06a Continued**



613

614 F06b

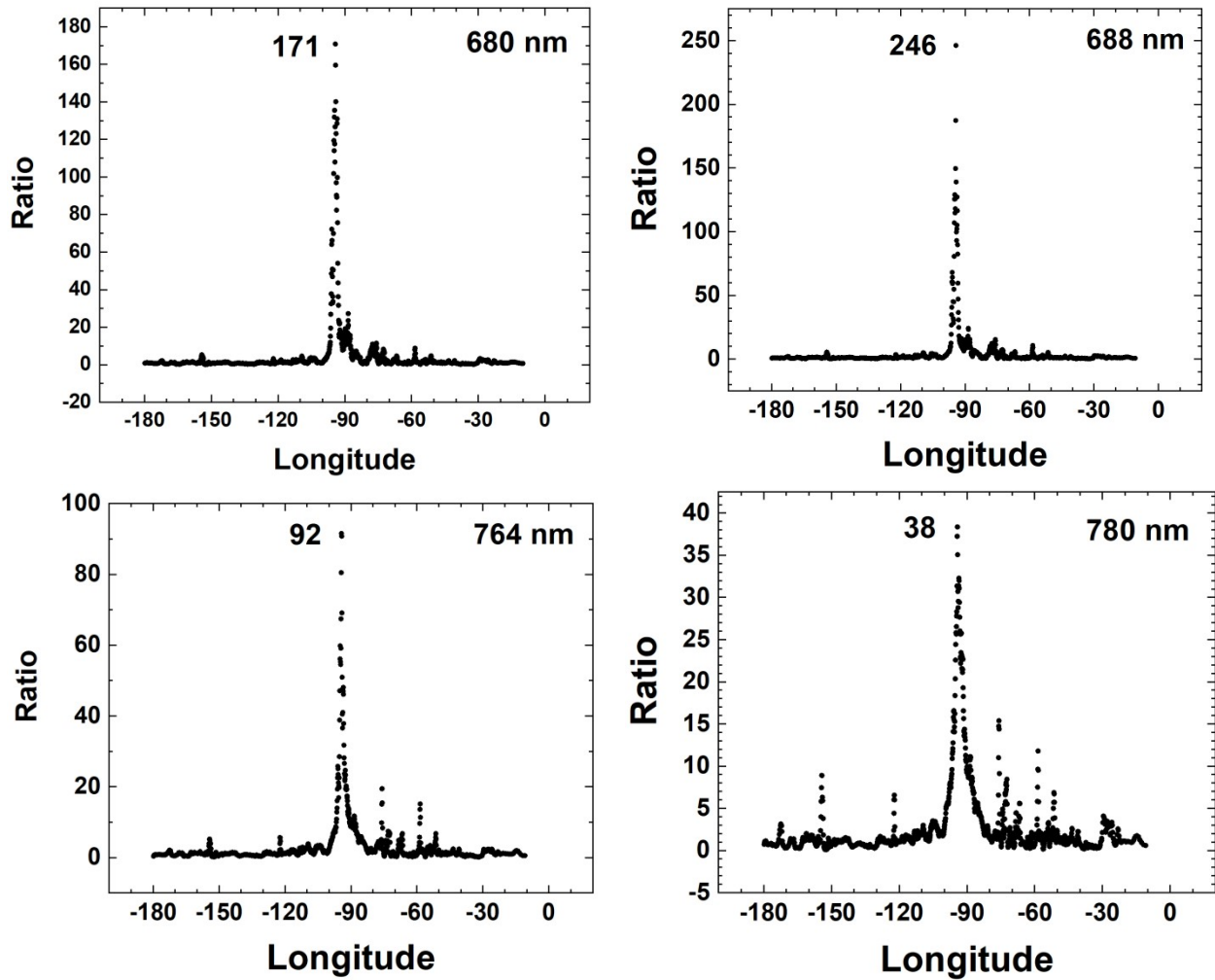


Fig. 6b. The ratio $R_{EN}(\lambda_i) = I(\text{Aug20})/I(\text{Aug21})$ at the time of the Eclipse in Columbia, Missouri for wavelengths 317.5 to 780 nm. The channels 317.5 to 340 nm are affected by ozone absorption and the channels 688 and 764 nm are within the O_2 B and A absorption bands.

615

616

617

618 **F06b Continued**

619

620

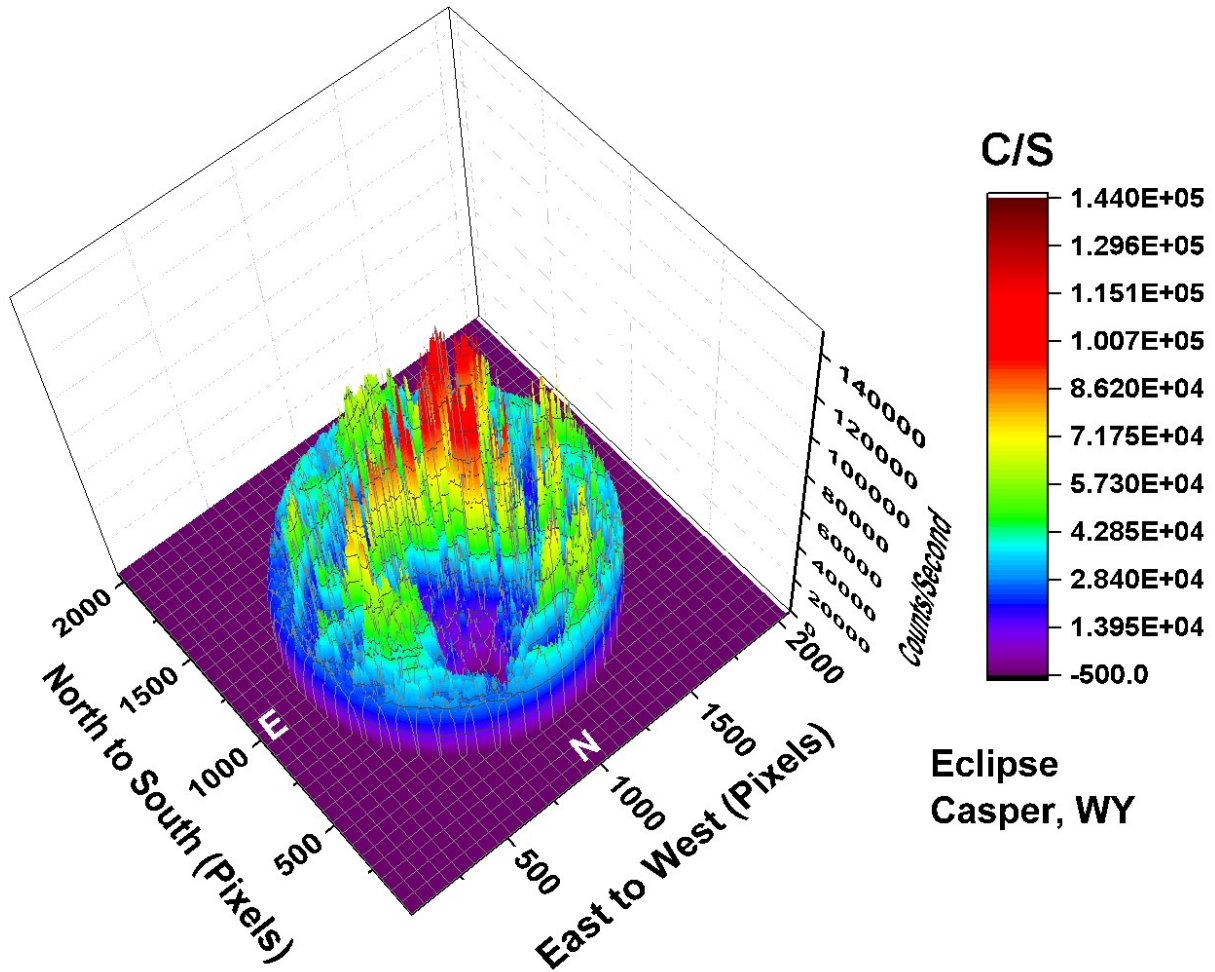


Fig. 7 The C/s observed by EPIC for the 443 nm channel corresponding to the color image shown in Fig. 1. In the data file, the word infinity has been replaced by the number zero. In this image there are approximately 2.59×10^6 illuminated pixels out of $2048^2 = 4.194304 \times 10^6$ pixels (61.8 %).

621

622

623 **F07**

624

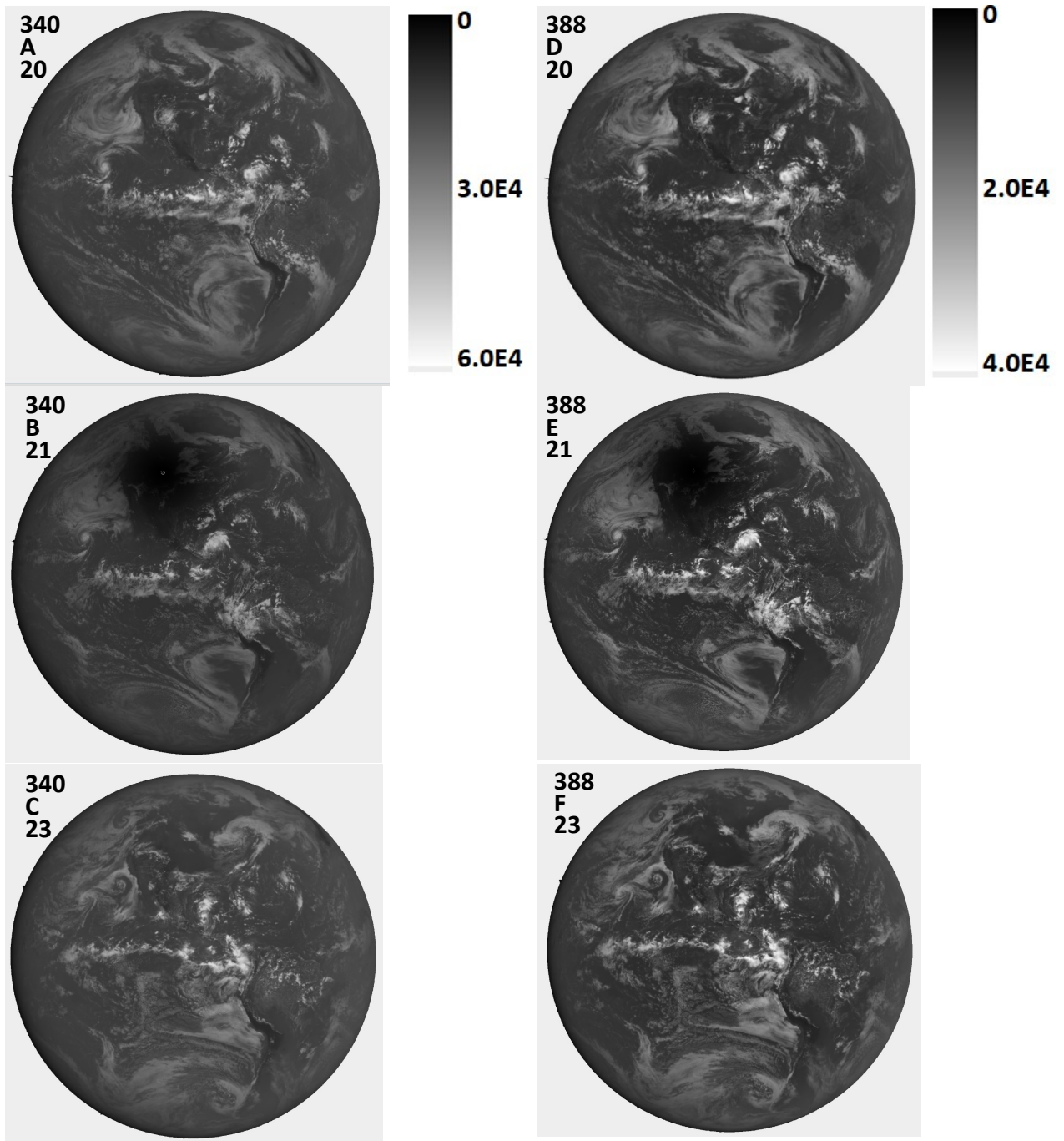


Figure 8a Image in C/s for 340 and 388 nm for 20 Aug.(A+C), 21 Aug. (B+E), and 23 Aug. (C+F). The scale applies to the specific wavelength. North is up.

625

F08a

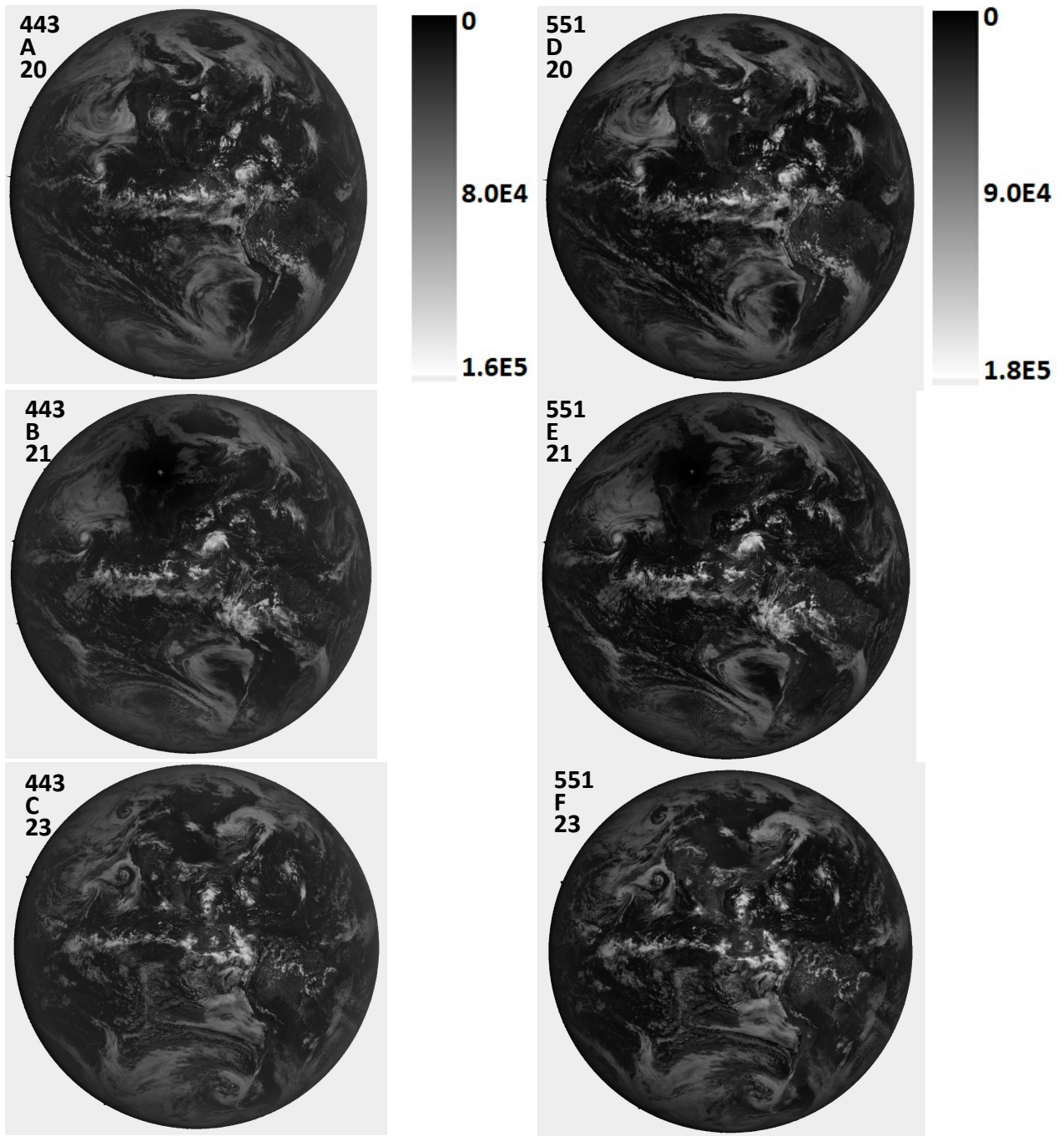


Figure 8b Image in C/s for 443 and 551 nm for 20 Aug.(A+C), 21 Aug. (B+E), and 23 Aug. (C+F). The scale applies to the specific wavelength. North is up.

626

627

628 **F08b**

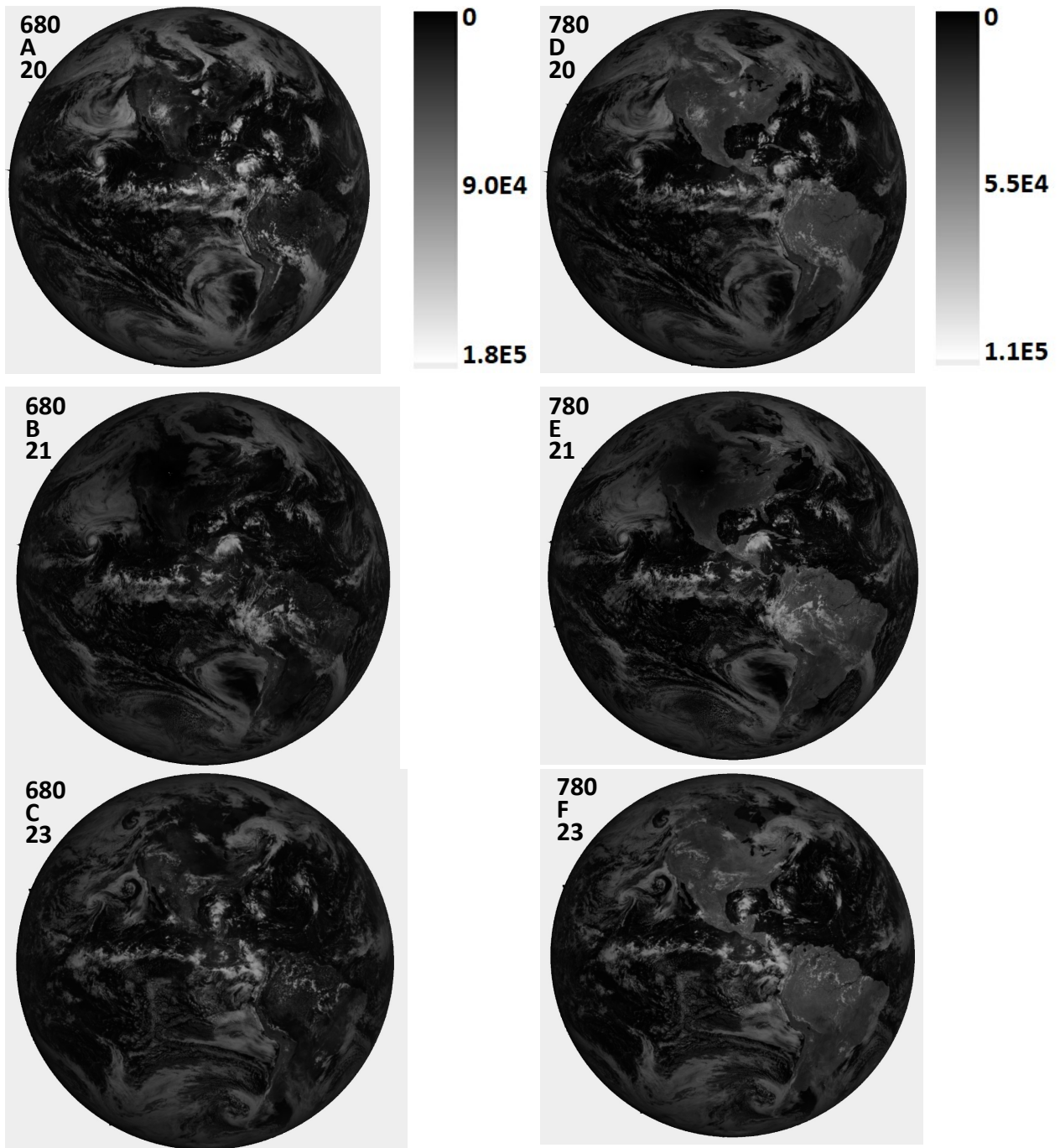


Figure 8c Image in C/s for 680 and 780 nm for 20 Aug.(A+C), 21 Aug. (B+E), and 23 Aug. (C+F). The scale applies to the specific wavelength. North is up.

629

630

631 **F08c**

632

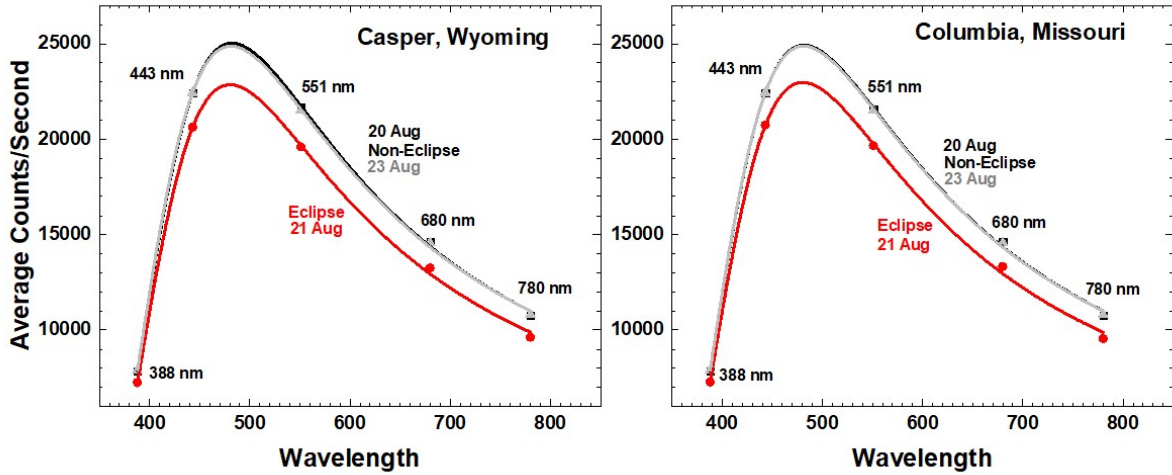


Fig. 9 Average reflected light in C/s for eclipse (21 Aug. red) and non-eclipse (20 Aug. and 23 Aug. (black and grey) days from Table 3 and Eqn. 1 for Casper and Columbia. The locations of the maxima are from curve fitting to the discrete wavelength measurements.

633

634

635 **F09**

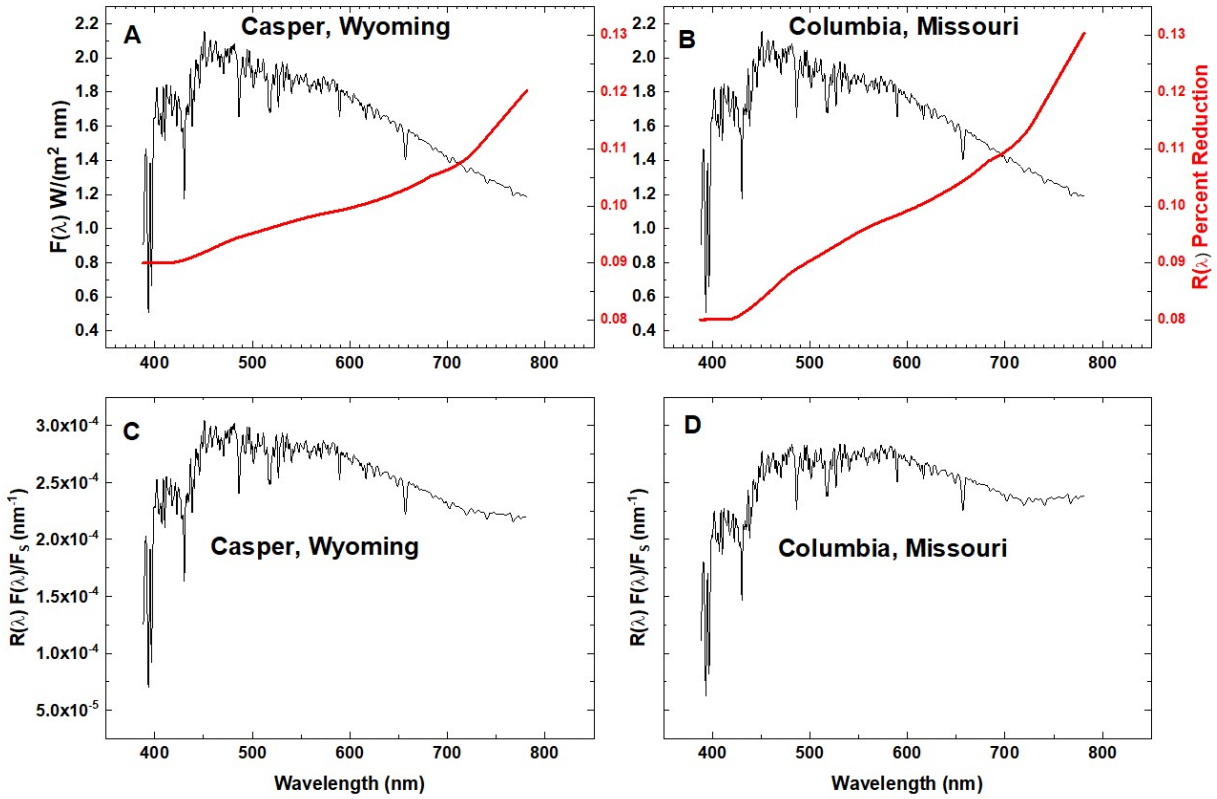


Fig. 10 Solar Irradiance at 1 AU $F(\lambda)$ Watts/(m^2 nm) (Mayer and Kylling, 2005) and the eclipse reduction function $R(\lambda)$ in percent for Casper, Wyoming (red curve in panel A) and Columbia, Missouri (red curve in panel B). Fractional reduction (nm^{-1}) in reflected solar irradiance in the direction of L-1 for Casper, Wyoming (panel C) and Columbia, Missouri (panel D)

636

637

638

639 **F10**

640

641

642

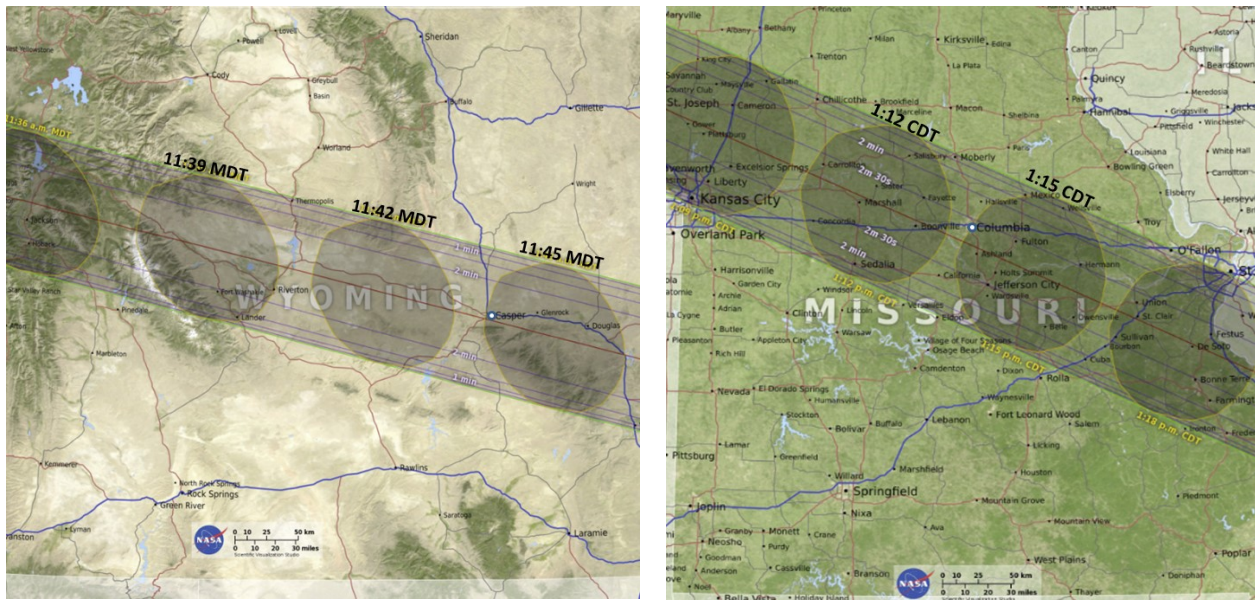


Fig. A1 The timing and shape of the Moon's shadow over Casper, Wyoming showing the relative location of Casper and Columbia (white circles) at 11:45 MDT (Mountain Daylight Time) and 1:15 CDT (Central Daylight Time). The shadow is moving at about 46 km/minute. (<https://eclipse2017.nasa.gov/eclipse-maps>). The NASA scale size is 50 km.

643

644

645

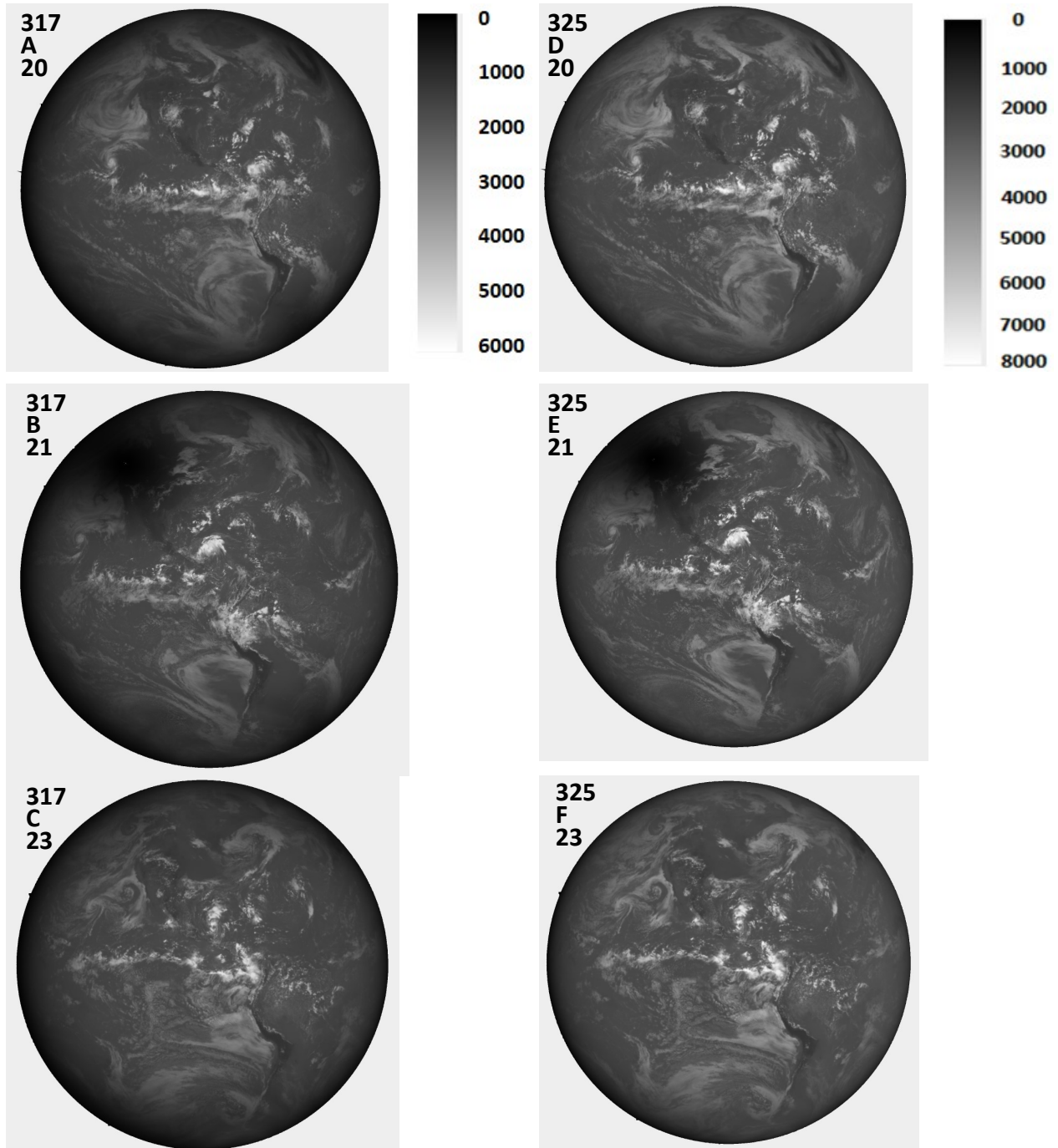


Fig. A2a Image in C/s for 317 and 340 nm for 20 Aug., 21 Aug. and 23 Aug. The scale applies to the specific wavelength. North is up.

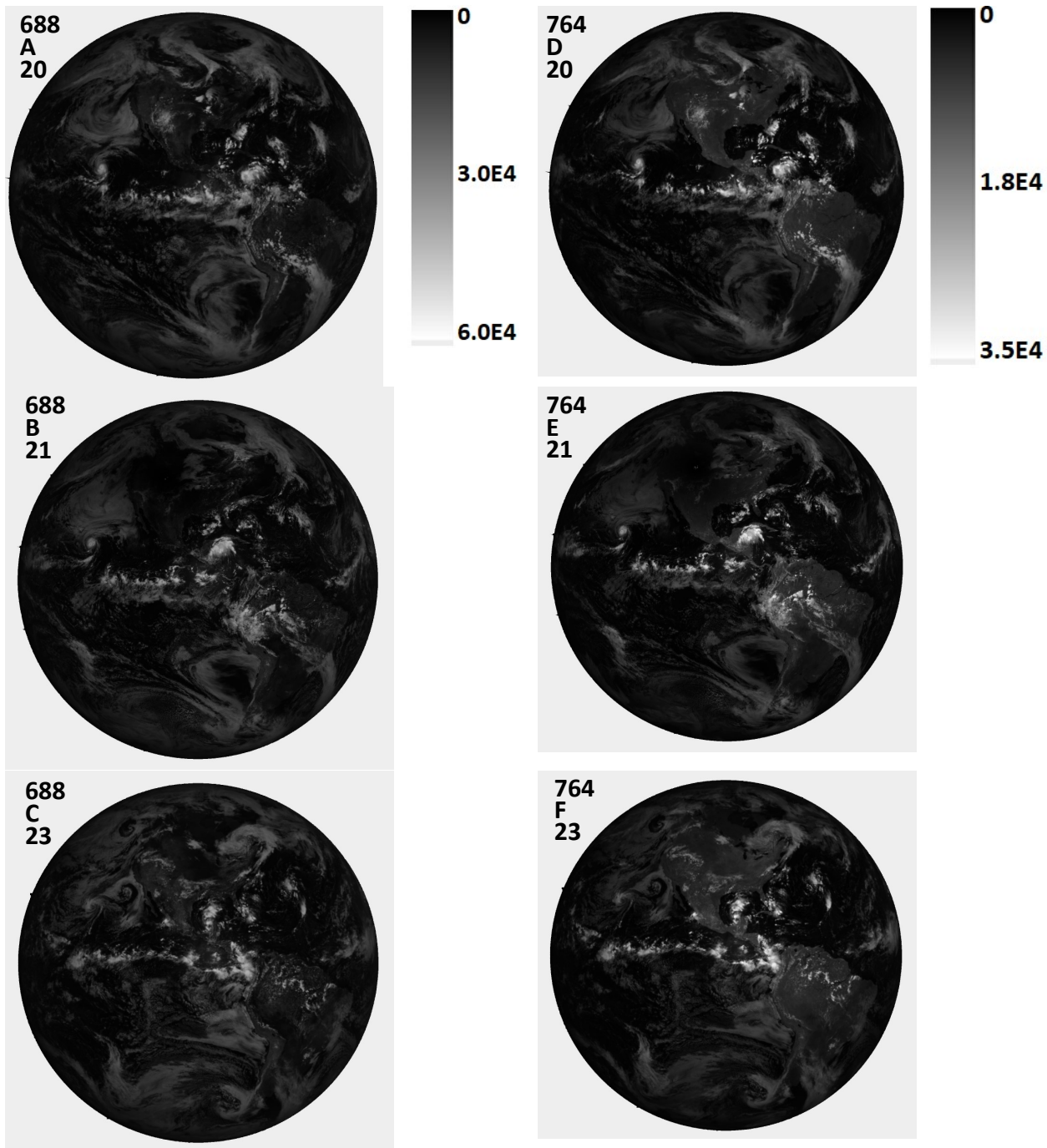


Fig. A2b Image in C/s for 688 and 764 nm for 20 Aug., 21 Aug. and 23 Aug. The scale applies to the specific wavelength. North is up.

650

651

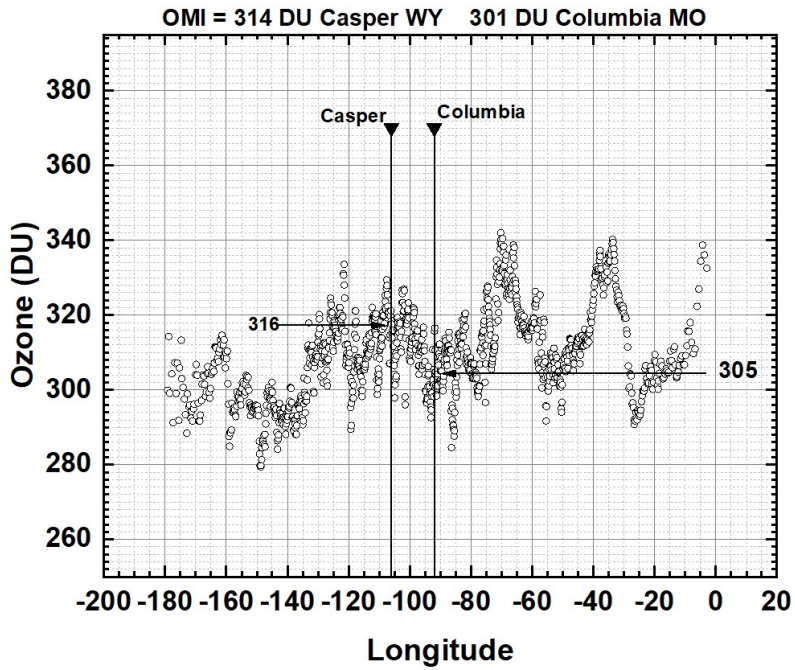


Fig. A3 EPIC measured ozone amounts from 20 August in the vicinity of Casper, WY and Columbia, MO.

652